

## Mapping Source-Specific Air Pollution Exposures Using Positive Matrix Factorization Applied to Multipollutant Mobile Monitoring in Seattle, WA

Ningrui Liu,\* Rajni Oshan, Magali Blanco, Lianne Sheppard, Edmund Seto, Timothy Larson, and Elena Austin



Cite This: *Environ. Sci. Technol.* 2025, 59, 3443–3458



Read Online

ACCESS |

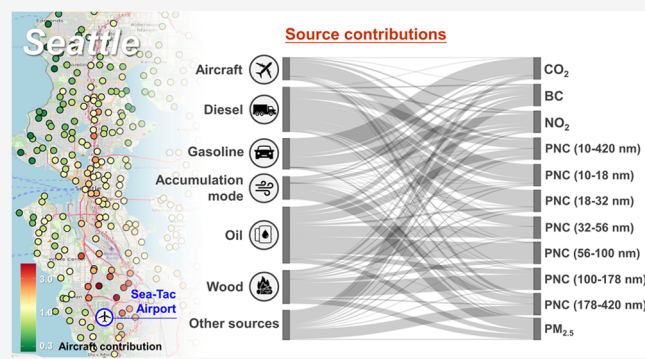
Metrics & More

Article Recommendations

Supporting Information

**ABSTRACT:** Mobile monitoring strategies are increasingly used to provide fine spatial estimates of multiple air pollutant concentrations. This study demonstrates a novel approach using positive matrix factorization (PMF) applied to multipollutant mobile monitoring data to assess source-specific air pollution exposures and to estimate associated emission factors. Data were collected from one-year mobile monitoring, with an average of 26 repeated measures of size-resolved particle number counts (PNC),  $\text{PM}_{2.5}$ , BC,  $\text{NO}_2$ , and  $\text{CO}_2$  at 309 sites in Seattle from 2019 to 2020. PMF was used to characterize underlying source-related factors. The sources associated with these six factors included emissions from aviation, diesel trucks, gasoline/hybrid vehicles, oil combustion, wood combustion, and accumulation mode aerosols. Fuel-based emission factors for three transportation-related sources were also estimated. This study reveals that PNC of ultrafine particles with size <18, 18–42, and 42–178 nm was dominated by features associated with aircraft, diesel trucks, and both oil and wood combustion. Gasoline and hybrid vehicles contributed the most to  $\text{CO}_2$  and  $\text{NO}_2$  concentrations. This approach can also be extended to other metropolitan areas, enhancing the exposure assessment in epidemiology studies.

**KEYWORDS:** air pollution, mobile monitoring, source apportionment, positive matrix factorization (PMF), exposure assessment, emission factor, ultrafine particles (UFP), black carbon (BC)



### 1. INTRODUCTION

Air pollution is associated with many adverse health outcomes, such as cardiovascular and respiratory diseases.<sup>1–5</sup> The Global Burden of Disease Study found that air pollution was the fourth leading risk factor globally, accounting for 8.4% of total disability-adjusted life years (DALYs).<sup>6</sup> Therefore, it is crucial to carefully quantify air pollution exposure and source contributions.

In the past decade, mobile monitoring campaigns have increasingly been adopted as a cost-effective approach to collect repeated measures of air pollutant concentrations at selected sites in the urban environment.<sup>7–16</sup> In such campaigns, researchers usually drive a vehicle equipped with high-quality instruments through an urban area. A few of these campaigns further consider measuring multiple air pollutants through fixed routes repeatedly during the sampling period. They measure the concentrations of targeted air pollutants while in motion or stopped along the road. Compared with traditional fixed air monitoring stations, mobile monitoring can provide a finer spatial resolution of air pollution exposures due to higher density of monitoring sites.<sup>17</sup> Mobile monitoring can

also provide enhanced spatial resolution of pollutants such as ultrafine particles (UFPs) and black carbon (BC), that are not usually collected at regulatory monitoring sites that focus on measurement of criteria air pollutants.<sup>18</sup> From a temporal perspective, although most of previous mobile monitoring campaigns have limited visit times of each site and restricted data collection periods, recent long-term mobile monitoring campaigns with time balanced design have been shown to better reflect annual average exposure to air pollution.<sup>19–22</sup>

Despite these advancements, current mobile monitoring studies still face limitations. Many studies focused on the mass concentration of fine particulate matter ( $\text{PM}_{2.5}$ ) and/or total particle number concentration (PNC), but recent evidence indicates that UFPs can have adverse health effects even at

Received: November 28, 2024

Revised: January 30, 2025

Accepted: January 31, 2025

Published: February 12, 2025



relatively low PM<sub>2.5</sub> mass concentrations.<sup>23,24</sup> The health impacts of particulate matter may be substantially influenced by the particle size distribution and chemical compositions of the particles, which depend on emission sources.<sup>25–28</sup> Additionally, the rich multipollutant spatiotemporal data of mobile monitoring campaigns, when collected, have not been fully utilized in health studies, and many studies still rely on single-pollutant health models. When multipollutant exposures are considered, researchers often encounter the challenge of high correlations between different air pollutants from common sources, which complicates statistical inference.<sup>29</sup> These reasons support the importance of characterizing the underlying sources of air pollution and estimating the exposure to source-specific air pollution. Moreover, a deeper understanding of air pollution sources can inform air quality management efforts aimed at controlling dominant emission sources to reduce health burdens.

Source apportionment studies have been previously conducted to identify unique sources of air pollution, especially for particulate matter. Hopke et al. performed comprehensive literature reviews on source apportionment of PM<sub>2.5</sub> and PM<sub>10</sub> based on chemical compositions and UFPs based on PNC in different size bins.<sup>30,31</sup> Some studies included in the reviews augmented the source apportionment with other gaseous pollutants such as nitrogen dioxide (NO<sub>2</sub>) and ozone. Many of these apportionment studies applied the positive matrix factorization (PMF) method, while others used principal component analysis (PCA), *k*-means clustering, and other similar algorithms.<sup>30,31</sup> Most of these studies have relied on data from fixed air monitoring stations, usually with lower spatial coverage and resolution than mobile monitoring campaigns. Recently, source apportionment models have been applied to mobile monitoring data which can overcome some of the above shortcomings.<sup>32–42</sup> (We denote studies using source apportionment with mobile monitoring as SA-MM studies in the following text.)

However, these SA-MM studies still have limitations. First, these studies typically considered gaseous pollutants or organic aerosol (OA) mass spectrometry measurements on their mobile platforms to characterize the sources of ambient air pollution. Few SA-MM studies considered particle size distribution,<sup>32,37</sup> even though it is known that particle size distribution is an important characteristic of different urban particle sources.<sup>43–45</sup> Second, classification of the transportation-related source into different vehicle types, such as aircraft, diesel trucks, and gasoline passenger vehicles is extremely limited, despite the significant role traffic-related air pollutants (TRAPs) play in air pollution exposure and corresponding health risks.<sup>1,4,46,47</sup> Actually, it is quite difficult to distinguish the emissions from different vehicle types using only the PMF or other receptor models. Third, few SA-MM studies have utilized land use regression (LUR) models to examine geospatial covariate correlations with factors identified by multivariate receptor models. For instance, a significantly positive association between source contribution and major road density suggests that this source is likely to be a road traffic-related source. Furthermore, most SA-MM studies have been constrained to limited time frames (from several days to several weeks), failing to capture the spatiotemporal variation of source contributions over an extended period.

Due to the importance of TRAPs, only a few SA-MM studies have further estimated the emission factors of different vehicle types.<sup>35,36,41</sup> These studies were based on source apportion-

ment using the absolute principal component score (APCS) model.<sup>35,36,41</sup> However, the APCS model, unlike PMF, does not consider measurement uncertainties and possible physical and chemical concentration constraints. Aside from SA-MM studies, other mobile monitoring studies focusing on emission factors either obtained total on-road emission factors without distinguishing different traffic sources,<sup>22,48,49</sup> or used “vehicle chase” strategies to measure the short-term emission factors of individual vehicles rather than the annual average emission factors at the regional level.<sup>41,50–53</sup>

Therefore, this study demonstrates an integrated method to address current gaps in source apportionment and emission factor estimation with mobile monitoring data capturing transportation-related air pollutants. By using multipollutant data from the quasi-stationary roadside measurements during one-year mobile monitoring campaign from the Adult Change in Thought Air Pollution (ACT-AP) study in the greater Seattle area, our approach aims to (1) characterize emission sources for various vehicle types; (2) assess source-related air pollution exposures; and (3) estimate the annual average emission factors for different vehicle types.

## 2. METHODS

**2.1. Multipollutant Data Collection.** The air pollution mobile monitoring campaign for the ACT study cohort has been introduced in detail in previous studies.<sup>20</sup> The selected mobile monitoring region was the Greater Seattle Area, WA, which has a population of 4.95 million in 2020 and a temperate climate and is known for its technology and aerospace industries. Briefly, this sampling campaign was conducted between March 2019 and March 2020 during all seasons and days of the week from 5 a.m. to 11 p.m. We used a hybrid vehicle to collect approximately 29 repeated 2 min measures of multiple pollutants, including size-resolved ultrafine particle number concentrations (with 13 size bins), PM<sub>2.5</sub>, BC, ultraviolet particulate matter (UVPM), NO<sub>2</sub>, and carbon dioxide (CO<sub>2</sub>) at 309 stationary sites at the side of the road (Figure S1 in the Supporting Information 1 (SI1)), representing residential locations of the ACT cohort. The mobile monitoring network design was carefully considered, including the number of stops and sample frequency.<sup>19</sup> Detailed instrument information is available in SI1 Table S1, including the measurement range, time resolution, and method detection limit (MDL). A series of quality assurance and quality control (QA/QC) procedures were performed, including the check of particle instruments for zero concentration responses, the calibration of gas instruments, the assessment of agreement between collocated instruments, the inspection of concentration pattern anomalies, and dropping data outside the instrument measurement range or with instrument error codes.<sup>20</sup> Finally, about 0.61% of the measurements were dropped.

As previously described, we used winsorized medians at the visit level to summarize each 2 min measurement for each air pollutant and reduce the impact of extreme measurements.<sup>20</sup> Specifically, we calculated the winsorized medians by setting values of the 2 min medians above the site-specific 95th percentile or below the fifth percentile to the corresponding threshold at the site level.<sup>20</sup> Approximately 10% of site visits with incomplete pollutant measurement data were excluded, resulting in a total of 8152 visits and an average of 26 visits per site retained. The minimum number of visits among all of the sites was 22. As most PNC measurements of the largest three

size bins (178–237, 237–316, and 316–420 nm) were found to be low, we summed PNCs of these three size bins into one (178–420 nm) for subsequent PMF analysis. Since our goal is to focus on the source contributions to air pollutants, we subtracted the CO<sub>2</sub> background concentration from the measured CO<sub>2</sub> concentration. The CO<sub>2</sub> background concentration was defined as the minimum measurement value during the mobile monitoring period of the visit day (a median of 4.4 h per day).<sup>22</sup> Hereafter, CO<sub>2</sub> will refer to this background-subtracted CO<sub>2</sub> concentration.

**2.2. Positive Matrix Factorization (PMF) Analysis.** As a widely used receptor model for source apportionment of air pollution, PMF decomposes the original sample data matrix ( $X$ ) into two separate matrices: a factor contribution matrix ( $G$ ) and a factor profile matrix ( $F$ ).<sup>54</sup> The model is

$$x_{ij} = \sum_{k=1}^K g_{ik} f_{kj} + e_{ij} \quad (1)$$

where  $x_{ij}$  is the concentration of species  $j$  in sample  $i$ ;  $g_{ik}$  is the contribution of factor  $k$  in sample  $i$ ;  $f_{kj}$  is the species profile of factor  $k$ , i.e., the concentration of species  $j$  in factor  $k$ ;  $e_{ij}$  is the residual; and  $K$  is the number of factors. The factor contribution and profile matrices are then obtained by solving the following constrained optimization problem.<sup>54</sup>

$$\begin{cases} G, F \end{cases} = \arg \min_{G, F} Q = \arg \min_{G, F} \sum_{i=1}^I \sum_{j=1}^J \frac{e_{ij}^2}{\sigma_{ij}^2}$$

$$\text{s.t. } g_{ik} \geq 0, f_{kj} \geq 0, \forall i = 1, 2, \dots, I; j = 1, 2, \dots, J;$$

$$k = 1, 2, \dots, K \quad (2)$$

where  $Q$  is the sum of squares of the residuals scaled by uncertainties;  $\sigma_{ij}$  is the uncertainty of concentration of species  $j$  in sample  $i$ ; and  $I$  and  $J$  are the number of samples and species, respectively.

We conducted all PMF analyses using the EPA PMF 5.0 software.<sup>54</sup> In this study, we used PMF in a spatiotemporal context. All 8125 visits to the 309 sites throughout one year were included, which means that the number of samples ( $I$  in eq 2) was 8125. A total of 18 species (i.e.,  $J = 18$  in eq 2) were input into the PMF model, including the total PNC (10–420 nm), PNC within 11 size bins, the ratio of PNC (36–1000 nm) to PNC (10–420 nm), PM<sub>2.5</sub>, NO<sub>2</sub>, BC, UVPM, and background-subtracted CO<sub>2</sub>. The concentration  $x_{ij}$  was modified by eq 3, and the corresponding uncertainty  $\sigma_{ij}$  was estimated by eq 4.<sup>54</sup>

$$\bar{x}_{ij} = \begin{cases} \frac{1}{2} \text{MDL}_j, & x_{ij} < \text{MDL}_j \\ x_{ij}, & x_{ij} \geq \text{MDL}_j \end{cases} \quad (3)$$

$$\sigma_{ij} = \begin{cases} \frac{5}{6} \text{MDL}_j, & x_{ij} < \text{MDL}_j \\ \sqrt{(\text{ErrF}_j \times x_{ij})^2 + (0.5 \text{MDL}_j)^2}, & x_{ij} \geq \text{MDL}_j \end{cases} \quad (4)$$

where MDL<sub>j</sub> is the method detection limit for species  $j$ ; and ErrF<sub>j</sub> is the error fraction of measuring concentrations of species  $j$ , which was determined by the median of relative error between the measurements of primary instrument and those of collocated back-up instruments. Detailed information on MDL<sub>j</sub>

and ErrF<sub>j</sub> are available in Table S1. In the EPA PMF 5.0 software, each pollutant needs to be categorized as “strong”, “weak”, or “bad” species according to its signal-to-noise ratio (S/N, available in Table S3).<sup>54</sup> Pollutants with S/N values ranging from 0 to 0.5 should be classified as “bad” and excluded from the PMF model. No pollutants were classified as “bad” in this study. Pollutants with S/N values ranging from 0.5 to 1.0 should be categorized as “weak”, and their uncertainty tripled, which included BC, UVPM, and PNC (178–420 nm) in this study. PNC (10–420 nm) was set as the total variable for UFP, which was automatically assigned as “weak”. Other pollutants were classified as “strong” species. EPA PMF 5.0 scales the  $G$  and  $F$  matrices to make the average contribution of each factor across all site visits equal to 1.

We determined the number of factors ( $K$ ) in this study according to several criteria:<sup>54</sup> (1) The  $Q/Q_{\text{exp}}$  should be smaller than 2, suggesting a good model fit, and  $K$  should be around the elbow point in the scree plot for  $Q/Q_{\text{exp}}$  (Note:  $Q_{\text{exp}} = IJ_{\text{strong}} - K(I + J_{\text{strong}})$ ,  $J_{\text{strong}}$  is the number of “strong” species); (2) The coefficient of determination ( $R^2$ ) between visit-level predictions and observations for “strong” species should be at least 0.6; (3) The accuracy of mapping bootstrap factors to base factors should be at least 80%; and (4) The resulting map of average factor contributions can be related to meaningful emission sources in the study region. Based on these criteria, we selected six factors in this study. Documentation of the detailed process can be found in SI1 Section S2.1.

After the PMF modeling, several diagnosis approaches were applied to ensure the reliability of the PMF results. We used  $G$ -space plots, the scatter plots of the factor contributions between each two factors, to check if there is collinearity between the factors. We performed the displacement (DISP) analysis to explore the rotational ambiguity of the PMF solution, where the counts of factor swaps and DISP intervals of the factor profile are provided.<sup>55,56</sup> In order to test the robustness of our results, we also randomly selected 155 sites out of the 309 sites (about 50%) for separate PMF analysis and calculated the correlation between the obtained profile and the original profile of each factor from the full data set. This random site selection test was repeated 10 times. A detailed description of these diagnosis approaches is available in SI1 Sections S2.2 and S2.3.

Finally, we obtained the factor profile ( $f_{kj}$ ) and factor contribution ( $g_{ik}$ ) from the PMF model. The mass concentration of brown carbon (BrC) was further obtained by subtracting BC from UVPM mass concentration from each factor profile, which is called as Delta-C approach.<sup>57–61</sup> We can then estimate the exposure level of pollutant  $j$  attributable to source  $k$  in sample  $i$  (denoted as  $x_{ijk}$ ) using eq 5 below.

$$x_{ijk} = g_{ik} f_{kj} \quad (5)$$

**2.3. External Validation and Factor Interpretation.** We simultaneously employed several methods in this study to help interpret the possible emission sources for each factor obtained from the PMF model. First, particle size distribution in each factor profile provides key information for source identification and was compared with previous studies about different emission source characteristics. Second, we obtained the average factor contributions at each site under different scenarios of various external variables, such as seasons, rush hours, wind directions, and ambient temperatures, to

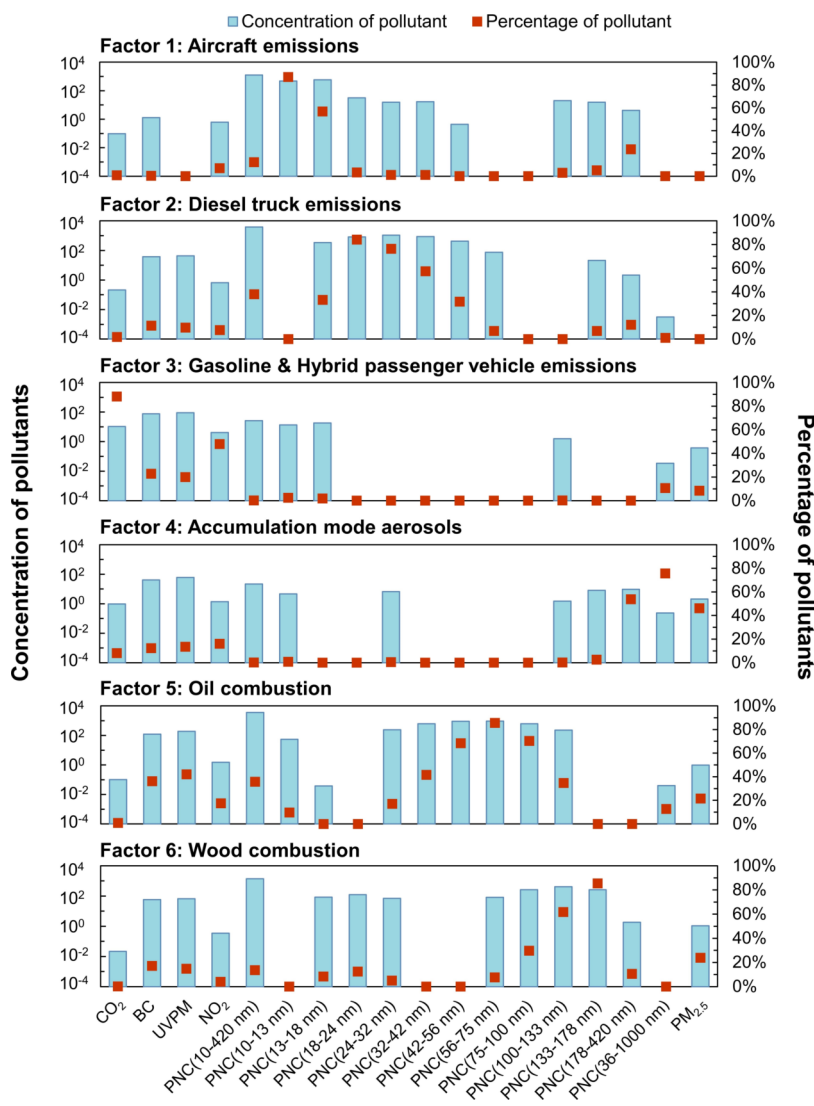


**Figure 1.** Profile of the six PMF factors, i.e., pollutant concentrations in each factor whose average contribution has been normalized to 1, and their percentage in total concentration of each pollutant. Note: The concentration unit is ppm for  $\text{CO}_2$ ,  $\text{ng}/\text{m}^3$  for BC, and UVPM, ppb for  $\text{NO}_2$ ,  $\#/ \text{cm}^3$  for size-resolved PNC, dimensionless for the ratio of PNC (36–1000 nm) to PNC (10–420 nm), and  $\mu\text{g}/\text{m}^3$  for  $\text{PM}_{2.5}$ . “PNC(36–1000 nm)” in the figure refers to the ratio of PNC (36–1000 nm) to PNC (10–420 nm).

investigate the associations between factor contributions and these variables. Seasons were classified as spring (March–May), summer (June–August), autumn (September–November), and winter (December–February). We defined rush hours as 7–10 a.m. and 4–7 p.m. on weekdays, while other hours were defined as nonrush hours. We acquired wind direction and temperature data at the Seattle-Tacoma International Airport from the Automated Surface Observing System (ASOS) Global METAR Archives of Iowa Environmental Mesonet.<sup>62</sup> In this study, a “north” wind was defined as a wind direction between 270 and 90°, while a “south” wind was between 90 and 270°. We then mapped the spatial distribution of average factor contributions under various scenarios to help interpret each of the factors as they relate to the underlying sources.

Third, to further inform the interpretation of each PMF factor, LUR models were used to identify associations between the annual average contribution of each PMF factor at each site and a comprehensive data set of geospatial covariates. The geospatial covariates included traffic-related data (e.g., road

density, distance to airports, distance to ports, and bus route density), urban structure-related data (e.g., elevation, proportion of different types of land use, and normalized difference vegetation index (NDVI)), other emission source-related data (e.g., the sum of major industrial emissions, residential building density, and fast food store density), and population density. Details of all geospatial covariates, including their definitions, metrics, data sources, and measurement methods, are available in SI1 Section S3. To identify more robust associations between PMF factors and geo-covariates, we employed two alternative model selection algorithms that are both capable of addressing multicollinearity among covariates: Elastic Net and partial least-squares (PLS). The Elastic Net algorithm combines the advantage of ridge and LASSO regression, and was used to select the covariates for each PMF factor, in which the penalty parameter and weight of ridge and LASSO part were determined by 10-fold cross-validation.<sup>29,63</sup> Then these selected covariates were included in a standardized linear regression model, and absolute values of regression coefficients among all statistically significant covariates were ranked to

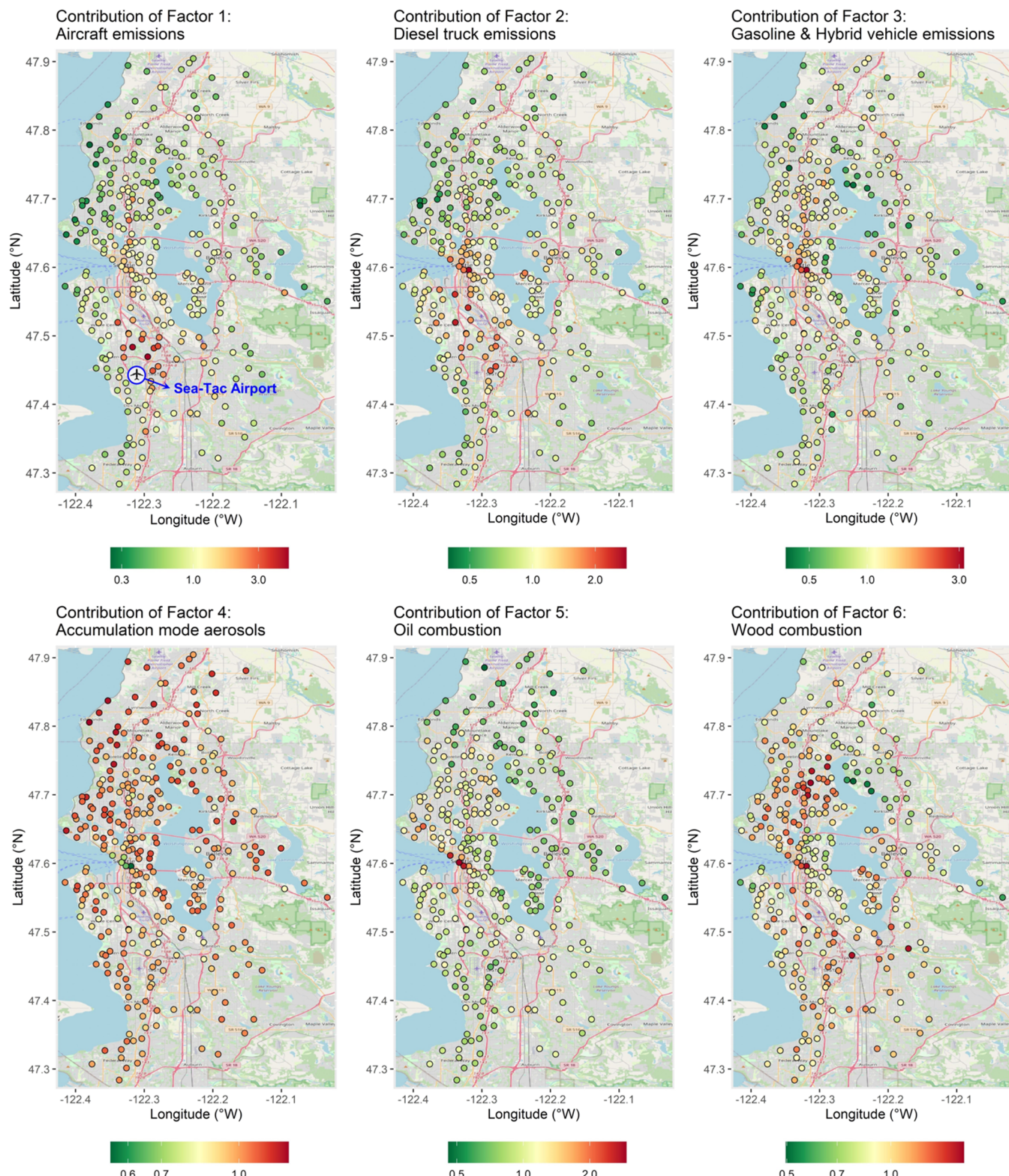


**Figure 2.** Annual average site-specific contributions (dimensionless) of the six PMF factors at the 309 stationary roadside sites from the Seattle mobile monitoring campaign. Different factors use different color scales to visually present the largest spatial variation. Note: The average contribution of each factor across all site visits is equal to 1 after scaling using EPA PMF 5.0 software. Therefore, Figure 2 can only be used to compare the source contributions in different sites within the same factor. Please use source-specific exposure in Table 1 to compare the contributions to one air pollutant between different factors.

identify the most influential covariates.<sup>64</sup> Additionally, PLS regression was fitted, with the number of components determined by 10-fold cross-validation as well.<sup>63</sup> The variable

importance in projection (VIP) score was applied to identify the top 10 influential geospatial covariates for each PMF

factor.<sup>65</sup> These identified influential covariates were then used to interpret the PMF factors.

Fourth, the ratios between concentrations of the selected species for each factor profile were calculated. These ratios included BC/CO<sub>2</sub>, BrC/CO<sub>2</sub>, NO<sub>2</sub>/CO<sub>2</sub>, PNC/CO<sub>2</sub> (for 10–420 nm), and PM<sub>2.5</sub>/BC. Usually, higher BrC/CO<sub>2</sub> indicates the source of biomass fuel burning,<sup>66,67</sup> and higher PM<sub>2.5</sub>/BC suggests the influence of secondary sources.<sup>68</sup> Among transportation-related sources, aircraft emission tends to have higher PNC/CO<sub>2</sub> because of generating more UFPs with 10–20 nm diameter for a given amount of fuel burned.<sup>69</sup> Diesel vehicles often have higher BC/CO<sub>2</sub>, NO<sub>2</sub>/CO<sub>2</sub>, and PNC/CO<sub>2</sub> than gasoline vehicles.<sup>70</sup>

**2.4. Emission Factors.** For transportation-related emission sources, source-specific fuel-based emission factors (EFs) can be estimated based on the ratios described in Section 2.3, using eq 6 below.<sup>69,71</sup>

$$\text{EF}_{j,k} = \frac{\Delta C_{j,k}}{\Delta \text{CO}_{2,k}} \times \omega \times 10^3 = \text{ratio} \times \frac{44}{12} \times \omega \times 10^3 \quad (6)$$

where EF<sub>j,k</sub> is the fuel-based EF of pollutant *j* for source *k*, g/kg fuel; ΔC<sub>j,k</sub> is the concentration of pollutant *j* in the profile of source *k*, g/m<sup>3</sup> (#/m<sup>3</sup> for PNC); ΔCO<sub>2,k</sub> is the background-subtracted CO<sub>2</sub> concentration in the profile of source *k*, g carbon/m<sup>3</sup>; and ω is the carbon mass fraction in the fuel, set as 0.85 in this study.<sup>49,72</sup> The 95% uncertainty interval was estimated through random site selection tests in Section 2.2. However, when compared with previous studies, some literature only reported the distance-based EF in g/mile. In this situation, we converted these distance-based EFs to fuel-based EFs according to the fuel efficiency (Details in SI1 Section S4). All spatial analysis and statistical analyses described in this section were performed with R V4.2.2 using the sf, sp, osmdata, stars, exactextractr, glmnet, pls, caret, vip, and stringr packages.<sup>73–84</sup>

### 3. RESULTS AND DISCUSSION

#### 3.1. Overview of Pollutant Concentrations and PMF Factors.

As shown in Table S6, the concentrations of air pollutants varied across different site visits and times. According to the coefficient of variation (CV, the ratio of standard deviation to mean), PNC within 10–13 and 13–18 nm had the largest variation (1.38 and 1.13), while PNC within 36–1000 nm and NO<sub>2</sub> had the smallest variation (0.70 and 0.71). Detailed annual average site-specific concentrations were mapped in previous studies,<sup>20</sup> suggesting that the pollutant concentrations were generally higher in urban areas than in suburban areas.

We identified a total of six factors from the PMF analysis. As can be seen from Figure S10, the correlations between PMF factor contributions were lower than those between air pollutant concentrations, suggesting that the multicollinearity of pollutant concentrations can be partly explained by the common emission sources. The G-space plots in Figure S3 and no factor swaps in the DISP analysis suggest that there is no significant rotational ambiguity in the PMF solution. The random site selection test demonstrates the robustness of the PMF solution, which shows a very high correlation of the factor profiles (>0.95 for almost all cases in Table S4) between the randomly selected data and original full data set. We categorized the six factors into three types, including

transportation-related sources (Factors 1, 2, and 3), accumulation mode aerosols (Factor 4), and oil and wood combustion sources (Factors 5 and 6). Their factor profiles and annual average site-specific factor contributions are illustrated in Figures 1 and 2, respectively. (Data are available in SI1 Table S7 and SI2 Table S14, respectively) Detailed interpretation and discussion of each factor will be described in Sections 3.2–3.4 below.

**3.2. Transportation-Related Sources.** Among transportation-related emission sources, factor 1 was related to aircraft emissions. As can be seen from the factor profile in Figure 1, factor 1 contributed 82.6 and 51.9% of UFPs for 10–13 and 13–18 nm among their total concentrations, respectively, which substantially outweighed other factors in this size range. The PNC/CO<sub>2</sub> of this factor was also much higher than factor 3 but a bit lower than factor 2 in Table S7. Previous field studies on air pollution monitoring at or near the airports have found that aircraft emissions are dominated by UFPs, 10–20 nm in size, which is smaller than the particle size of road traffic emissions, and consistent with the characteristics of factor 1.<sup>71,85–92</sup> Additionally, some studies found a bimodal distribution of particle size from aircraft emissions, which peaks at 10–20 nm and at approximately 100–150 nm.<sup>85,93</sup> The profile of factor 1 shows a similar size distribution, with considerable contribution from UFPs for 100–178 nm. Furthermore, the spatial distribution of the annual average site-specific contribution of factor 1 helped identify factor 1 as aircraft emissions. No significant differences in the spatial pattern were found between different seasons (Figure S11) or between rush and nonrush hours (Figure S12). Figure 2 suggests that the factor contribution was higher around Seattle-Tacoma International Airport. The quantitative LUR models (both Elastic Net and PLS regression model) indicated that the distance to large airports and the air routes are important covariates and negatively associated with the factor contribution (Table S8). Among these important covariates, the distance to the north landing route has the strongest association. This can be further supported by the covariance between factor contribution and wind directions, consistent with previous studies.<sup>71,85,86,90,91,94–101</sup> As shown in Figure S13, under the south wind, the factor contribution was significantly higher downwind, i.e., the north of the airport under the landing path. By contrast, the impact of aircraft emission under the north wind prevailing in the summer was not so obvious in Figure S13, partly due to the scarcity of mobile monitoring sites to the south of the airport.

We characterized factors 2 and 3 as road traffic emission sources, which are usually considered to be dominated by UFPs of size 30–50 nm.<sup>91</sup> We considered factor 2 to be associated with diesel truck emissions. The particle size of factor 2 was enriched in 13 to 75 nm and peaked at 24–32 nm, which is larger than factors 1 and 3. The particle size distribution of diesel truck emission varied widely in previous studies, ranging from 10 to 100 nm, based on whether the truck uses diesel particle filters (DPF) and selective catalytic reduction (SCR) and whether it is light-duty or heavy-duty.<sup>102–105</sup> For instance, Ban-Weiss et al. reported that the PNC of heavy-duty trucks peaked at 16 nm and light-duty trucks at 22 nm.<sup>102</sup> Some of these studies reported a bimodal or trimodal size distribution, which represents the nucleation and accumulation mode of particles.<sup>103,105</sup> We have not observed a multimodal size distribution in the profile of factor 2, but the size distribution is consistent with the reported

values in the literature. From the spatial distribution shown in Figure 2, higher factor contributions can be found around the Seattle downtown area, the airport, and the industrial district between the two above, which require trucks for freight transport. The LUR models also selected primary road density, distance to large airport and air routes, and proportion of industrial land use and developed high-intensity landcover as influential geospatial covariates (Table S9). Furthermore, from the perspective of ratios, a higher BC/CO<sub>2</sub> than factor 1 and insignificant differences under different wind directions (Figure S16) ruled out the possibility that factor 2 represents the aging particles emitted from aircraft. The BC/CO<sub>2</sub>, NO<sub>x</sub>/CO<sub>2</sub>, and PNC/CO<sub>2</sub> ratios of factor 2 were significantly higher than that of factor 3 (Table S7). It suggests that factor 2 may be attributable to diesel vehicle emissions instead of gasoline emissions, which will be further validated through emission factors in Section 3.6.

We considered factor 3 to be influenced by gasoline and hybrid passenger vehicle emission sources, such as cars and buses. The particle size distribution was abundant in 10 to 18 nm, but the DISP intervals also showed particle size distribution larger than 18 nm. Previous studies found that particles emitted from gasoline vehicles usually have a peak around 10–20 nm, which agrees well with the feature of factor 3.<sup>106–111</sup> From the spatial perspective, the annual average contribution of factor 3 was much higher in the downtown area and along the I-5 and SR-99 Highways (Figure S17). We identified road density, bus route density, and the distance to bus routes as important covariates in the LUR models (Table S10). We note that most buses in King County are electric-diesel hybrid or electrical buses, so they emit much less NO<sub>x</sub> and particles than traditional diesel buses.<sup>112</sup> In addition, since the bus route density considered the number of bus routes in one road segment (e.g., Bus No. 31 and No. 65) rather than the total length of roads with busways, higher bus route density can, to some extent, represent higher traffic volume of passenger cars on this road based on the principles of public transportation design. From the temporal perspective, the factor contributions were the highest in winter and the lowest in summer (Figure S17), which may result from the presence of particles with semivolatile physicochemical properties.<sup>113</sup> Higher factor contributions were also found within rush hours than nonrush hours (Figure S18), which corresponds with the pattern of passenger cars and buses.

**3.3. Accumulation Mode Aerosols.** Since the PM<sub>2.5</sub>/BC ratio for factor 4 is much higher than other factors and the particles with size larger than 100 nm dominate the factor profile, factor 4 is likely to be accumulation mode aerosols coagulated from finer particles and secondary aerosols, rather than primary emission sources.<sup>31,68</sup> We observed no significant differences in its contribution between different seasons or between rush and nonrush hours from Figures S19 and S20. However, we found a higher contribution of factor 4 farther away from downtown Seattle and the I-5/SR-99 Highway. This interpretation was further supported by the LUR model results in Table S11, which show that the factor contribution was significantly negatively associated with primary road density and bus route density and positively associated with the distance to primary roads and bus routes. All the above evidence implies that factor 4 refers to the accumulation mode aerosols, which mainly come from vehicle primary emissions transported from city centers and primary roads to suburban areas.

**3.4. Oil and Wood Combustion Sources.** We initially categorized factors 5 and 6 as sources related to biomass fuel burning because their BrC/CO<sub>2</sub> ratios were much higher than those of the other four factors. Previous studies indicate that residential heating generates a particle size distribution with the mode around 90 to 100 nm, which the profiles of factors 5 and 6 cover.<sup>31</sup> Previous studies also suggest that the wood and oil combustion from residential heating accounted for a large proportion of UFP pollution in Seattle.<sup>114,115</sup> Therefore, these two factors are likely related to residential heating emissions. There are differences between these two factors, though, as discussed separately below.

As can be seen from Figures S21 and S22, the contribution of factor 5 had no significant difference between rush and nonrush hours, but was much higher in autumn and winter. In order to explore the seasonal difference, we estimated the factor contributions at different ambient temperature intervals (Figure S23). When the temperature was lower than 5 °C, there were extremely high factor contribution in the northern region of the Greater Seattle Area, which is likely the result of residential heating emissions. Nevertheless, we also found higher contributions nearby the port of downtown Seattle at higher temperatures. In Table S12, the LUR model with the Elastic Net algorithm identified house density as a significant positive covariate, which is consistent with the fact that biomass fuels and natural gas tend to be used in houses and electricity in apartments. From the American Community Survey (ACS) estimates, it can be found that the number of households using heating oil as heating fuels in the northern area was much more than other regions (Figure S24), suggesting that heating oil combustion may explain the high contribution of factor 5.<sup>116</sup> Additionally, the distance to ports, fast food store density, and restaurant density were selected as important covariates for contribution of factor 5, which represent the emission from ship fuel burning and cooking in restaurants and explain the high contribution in the downtown area. In 2013, 77% of marine ship fuels used heavy fuel oil, the typical residual fuel oil including No.5 and No.6 Fuel Oil.<sup>117</sup> Cooking oil fumes have been found to contribute substantial particle exposures during cooking even with clean fuel.<sup>118,119</sup> However, ship emissions are likely the most important source for factor 5 when ambient temperatures are moderate to high, although we find correlations between this factor and spatial distributions of restaurants and might hypothesize cooking emission contributions. That is because cooking in restaurants and fast food establishments usually contributes much more to indoor air pollution than to outdoor air pollution. All the above evidence suggests that factor 5 may be oil combustion from residential heating and ship emissions.

We identified factor 6 as wood combustion emissions, which is a second type of residential heating. The temporal patterns of contributions of factor 6 in Figures S25 and S26 were similar to factor 5, with higher contributions observed in autumn and winter, but no significant differences between rush and nonrush hours. Figure S27 demonstrates that factor 6 had higher contributions in the northern and southeastern suburban areas of Seattle only when the temperature was lower than 5 °C. Therefore, factor 6 is likely from the residential heating emission sources. The LUR models did not only select geo-covariates such as house density, but also identified the sum of NO<sub>x</sub>, SO<sub>2</sub>, PM<sub>2.5</sub>, and PM<sub>10</sub> of major industrial emissions, the proportion of industrial land use, and the distance to truck routes as important covariates (Table

**Table 1.** Mean  $\pm$  Standard Deviation (Percentage) of Annual Average Source-Specific Air Pollution Exposure across 309 Sites in the Greater Seattle Area<sup>a</sup>

pollutant	factor 1	factor 2	factor 3	factor 4	factor 5	factor 6	total
CO <sub>2</sub> (ppm)	0.1 $\pm$ 0.1 (0.7%)	0.2 $\pm$ 0.1 (1.6%)	10.5 $\pm$ 3.6 (74.5%)	1.0 $\pm$ 0.1 (0.8%)	0.0 $\pm$ 0.0 (0.2%)	11.9 $\pm$ 3.6 (85.7%)	
BC (ng/m <sup>3</sup> )	1.3 $\pm$ 0.8 (0.2%)	38.2 $\pm$ 14.1 (7.0%)	76.8 $\pm$ 26.5 (13.8%)	41.7 $\pm$ 4.0 (8.1%)	121.7 $\pm$ 37.8 (22.1%)	57.6 $\pm$ 11.7 (10.7%)	337.2 $\pm$ 67.9 (61.8%)
UVPM (ng/m <sup>3</sup> )	0.0 $\pm$ 0.0 (0.0%)	43.5 $\pm$ 16.0 (6.9%)	89.5 $\pm$ 30.9 (14.0%)	60.6 $\pm$ 5.8 (10.3%)	186.9 $\pm$ 58.0 (29.4%)	66.3 $\pm$ 13.5 (10.7%)	446.7 $\pm$ 90.2 (71.2%)
NO <sub>2</sub> (ppb)	0.6 $\pm$ 0.4 (6.5%)	0.6 $\pm$ 0.2 (7.0%)	4.1 $\pm$ 1.4 (44.2%)	1.4 $\pm$ 0.1 (16.2%)	1.5 $\pm$ 0.5 (16.3%)	0.3 $\pm$ 0.1 (3.9%)	8.6 $\pm$ 1.9 (94.3%)
total PNC (10–420 nm) (#/cm <sup>3</sup> )	1255 $\pm$ 777 (11.5%)	3854 $\pm$ 1420 (36.6%)	26 $\pm$ 9 (0.2%)	22 $\pm$ 2 (0.2%)	3608 $\pm$ 1121 (35.2%)	1377 $\pm$ 281 (13.6%)	10141 $\pm$ 2645 (57.5%)
PNC (10–13 nm) (#/cm <sup>3</sup> )	484 $\pm$ 300 (82.6%)	0 $\pm$ 0 (0.0%)	14 $\pm$ 5 (2.7%)	5 $\pm$ 0 (1.0%)	54 $\pm$ 17 (11.3%)	0 $\pm$ 0 (0.0%)	556 $\pm$ 302 (97.6%)
PNC (13–18 nm) (#/cm <sup>3</sup> )	578 $\pm$ 358 (51.9%)	336 $\pm$ 124 (33.0%)	18 $\pm$ 6 (1.9%)	0 $\pm$ 0 (0.0%)	85 $\pm$ 17 (9.1%)	1017 $\pm$ 461 (95.9%)	
PNC (18–24 nm) (#/cm <sup>3</sup> )	32 $\pm$ 20 (3.0%)	818 $\pm$ 301 (79.9%)	0 $\pm$ 0 (0.0%)	0 $\pm$ 0 (0.0%)	0 $\pm$ 0 (0.0%)	121 $\pm$ 25 (13.0%)	971 $\pm$ 323 (95.9%)
PNC (24–32 nm) (#/cm <sup>3</sup> )	15 $\pm$ 10 (1.0%)	1079 $\pm$ 398 (72.8%)	0 $\pm$ 0 (0.0%)	7 $\pm$ 1 (0.5%)	240 $\pm$ 75 (17.2%)	71 $\pm$ 14 (5.1%)	1412 $\pm$ 434 (96.6%)
PNC (32–42 nm) (#/cm <sup>3</sup> )	17 $\pm$ 11 (1.1%)	862 $\pm$ 318 (54.2%)	0 $\pm$ 0 (0.0%)	0 $\pm$ 0 (0.0%)	622 $\pm$ 193 (40.3%)	0 $\pm$ 0 (0.0%)	1501 $\pm$ 418 (95.5%)
PNC (42–56 nm) (#/cm <sup>3</sup> )	0 $\pm$ 0 (0.0%)	422 $\pm$ 156 (30.8%)	0 $\pm$ 0 (0.0%)	0 $\pm$ 0 (0.0%)	908 $\pm$ 282 (65.8%)	0 $\pm$ 0 (0.0%)	1330 $\pm$ 356 (96.6%)
PNC (56–75 nm) (#/cm <sup>3</sup> )	0 $\pm$ 0 (0.0%)	75 $\pm$ 28 (7.0%)	0 $\pm$ 0 (0.0%)	0 $\pm$ 0 (0.0%)	932 $\pm$ 289 (84.1%)	83 $\pm$ 17 (7.8%)	1089 $\pm$ 306 (98.9%)
PNC (75–100 nm) (#/cm <sup>3</sup> )	0 $\pm$ 0 (0.0%)	0 $\pm$ 0 (0.0%)	0 $\pm$ 0 (0.0%)	0 $\pm$ 0 (0.0%)	618 $\pm$ 192 (67.4%)	263 $\pm$ 54 (29.6%)	881 $\pm$ 221 (96.9%)
PNC (100–133 nm) (#/cm <sup>3</sup> )	20 $\pm$ 13 (3.0%)	0 $\pm$ 0 (0.0%)	2 $\pm$ 1 (0.2%)	1 $\pm$ 0 (0.2%)	229 $\pm$ 71 (33.6%)	410 $\pm$ 84 (60.8%)	663 $\pm$ 135 (97.9%)
PNC (133–178 nm) (#/cm <sup>3</sup> )	16 $\pm$ 10 (4.7%)	21 $\pm$ 8 (6.5%)	0 $\pm$ 0 (0.0%)	8 $\pm$ 1 (2.6%)	0 $\pm$ 0 (0.0%)	261 $\pm$ 53 (80.2%)	306 $\pm$ 59 (94.0%)
PNC (178–420 nm) (#/cm <sup>3</sup> )	4 $\pm$ 3 (14.8%)	2 $\pm$ 1 (8.1%)	0 $\pm$ 0 (0.0%)	9 $\pm$ 1 (38.2%)	0 $\pm$ 0 (0.0%)	2 $\pm$ 0 (7.4%)	18 $\pm$ 3 (68.4%)
PM <sub>2.5</sub> (µg/m <sup>3</sup> )	0.0 $\pm$ 0.0 (0.0%)	0.0 $\pm$ 0.0 (0.0%)	0.4 $\pm$ 0.1 (8.1%)	2.1 $\pm$ 0.2 (45.4%)	1.0 $\pm$ 0.3 (20.3%)	1.1 $\pm$ 0.2 (22.9%)	4.5 $\pm$ 0.4 (96.6%)

<sup>a</sup>Note: The sum of pollutant-specific percentages across the six factors may be smaller or larger than 100%, because the PMF model has residuals, suggesting that there are additional sources contributing to the pollutant concentrations besides these six factors.

**Table 2.** Fuel-Based Emission Factors (g/kg Fuel) of Transportation-Related Sources in This Study and the Previous Literature

pollutant		aircraft	diesel truck	gasoline and hybrid passenger vehicle
BC	this study	$2.3 \times 10^{-2}$ (0–8.7 × 10 <sup>-2</sup> ) <sup>a</sup>	$3.1 \times 10^{-1}$ (3.1 × 10 <sup>-1</sup> –6.6 × 10 <sup>-1</sup> )	$1.3 \times 10^{-2}$ (1.1 × 10 <sup>-2</sup> –1.4 × 10 <sup>-2</sup> )
	literature	$4.2 \times 10^{-2}$ [Global] <sup>122</sup>	1.1 (GM)/1.7 (AM) [CA, USA] <sup>124b</sup> 1.1 (no DPF)/1.1 × 10 <sup>-1</sup> (DPF) [CA, USA] <sup>127</sup>	$1.7 \times 10^{-2}$ <sup>126</sup>
NO <sub>x</sub>	this study	20 (8.0–20)	9.9 (8.5–20)	1.3 (1.2–1.3)
	literature	14 [Global] <sup>122c</sup> 9.1 (land)/34 (takeoff) [USA] <sup>123c</sup>	9.5 [USA] <sup>125c</sup> 1.1 (no DPF)/2.1 (DPF) [CA, USA] <sup>127</sup>	2.0 [USA] <sup>125c</sup> 1.6 [WA, USA] <sup>112c</sup>
PNC	this study	$2.2 \times 10^{16}$ $(9.6 \times 10^{15}–2.6 \times 10^{16})$	$3.1 \times 10^{16}$ (3.1 × 10 <sup>16</sup> –7.8 × 10 <sup>16</sup> )	$4.3 \times 10^{12}$ (1.6 × 10 <sup>11</sup> –7.7 × 10 <sup>12</sup> )
	literature	$3.8 \times 10^{16}$ [CA, USA] <sup>89</sup>	$2.8 \times 10^{15}$ (GM)/ $4.7 \times 10^{15}$ (AM) [CA, USA] <sup>124</sup> $7.7 \times 10^{15}$ (no DPF)/ $1.0 \times 10^{16}$ (DPF) [CA, USA] <sup>127</sup>	$2.2 \times 10^{13}$ [Finland] <sup>109</sup> 9.9 × 10 <sup>13</sup> [Finland] <sup>128</sup>

<sup>a</sup>The values in the brackets represent the 95% uncertainty interval of the estimated emission factors in this study. <sup>b</sup>GM and AM refer to geometric and arithmetic mean. <sup>c</sup>Only NO<sub>x</sub> emission factor was available in this paper.

S13). According to ACS estimates of household income,<sup>116</sup> the correlation between household income and proportion of industrial land use within 1, 3, 5, and 10 km of census block groups in Seattle was estimated as –0.16, –0.30, –0.37, and –0.41, respectively. It suggests that there are usually more low-income households in the vicinity of industrial land use possibly due to environmental pollution, which cannot afford high-price clean heating fuels. However, due to the difference in particle size and spatial distribution between factor 5 and this factor, the specific residential heating fuels should be different as well. The ACS estimates demonstrate that a larger number of households using wood as residential heating fuel exists in the southeastern area of Seattle (Figure S28), which probably influenced the eastern and southeastern urban area under the prevailing south wind in winter.<sup>116</sup> Besides, the reported particle size distribution in previous field studies on residential wood combustion is consistent with the profile of factor 6. The particles from some types of woodstoves were found to have a monomodal size distribution of 180–200 nm in the start-up and steady-state phases, but have a bimodal distribution of 30–60 and 180–200 nm in the burn-out phase.<sup>120</sup> Also, fireplaces and masonry heaters have been found to generate high particle emissions at 10–30 and 70–326 nm.<sup>120</sup> Similarly, this factor contributed PNC within 13–32 and 56–420 nm. Therefore, we considered factor 6 as the wood combustion from residential heating.

**3.5. Source-Specific Air Pollution Exposure Assessment.** Besides the annual average factor contribution in Figure 2, the exposure levels to various air pollutants attributable to these sources can be further obtained; these are summarized in Table 1 and shown at each site in SI2 Table S15. Background-subtracted CO<sub>2</sub> was dominated by emissions from gasoline and hybrid passenger vehicles (factor 3), which accounted for 74.5% of total CO<sub>2</sub> emissions and elevated the annual average CO<sub>2</sub> concentration by 10.5 ppm. Similar results can be found for NO<sub>2</sub> that factor 3 generated 44.2% of the total NO<sub>2</sub> emissions and ranked first among all identified sources. For BC and UVPM, oil combustion from residential heating, ship, and cooking in restaurants and fast food establishments (factor 5) contributed the most (22.1 and 29.4%), followed by gasoline and hybrid vehicle emissions (factor 3, 13.8 and 14.0%). For total PNC within 10–420 nm, oil and wood combustion sources (factors 5 and 6) accounted for 48.8%, followed by 36.6% from diesel truck emissions. A previously published review shows that heating and transportation-related sources contributed 48 and 20% of total PNC (20–400 nm) emissions,

respectively, which is consistent with our findings.<sup>31</sup> However, the source contribution can vary a lot for different particle sizes. The oil and wood combustion sources provided the largest emission contributions for PNC within 56–75 nm (91.9%) and 75–100 nm (97.0%), whereas the diesel truck emissions contributed the most for PNC within 18–24 nm (79.9%) and 24–32 nm (72.8%). Although aircraft emissions (factor 1) contributed only 11.5% of the total PNC, it accounted for 82.6 and 51.9% of PNC emissions within 10–13 and 13–18 nm, respectively, suggesting the critical role of aircraft in the exposure to the smallest ultrafine particles. In contrast, gasoline and hybrid vehicles account for less than 5% for all size bins of PNC in this study. For the mass concentration of PM<sub>2.5</sub> which represents large particles, accumulation mode aerosols from transportation outweighed other sources and contributed 45.4%. Friedman found that through PMF analysis of PM<sub>2.5</sub> chemical compositions at one monitoring station in downtown Seattle, gasoline and diesel traffic sources can contribute 50% of PM<sub>2.5</sub> pollution, which agrees with the results of this study.<sup>121</sup> Furthermore, the total contributions of six sources contributed more than 85% of the measured concentrations for most pollutants, except for the three “weak” pollutants (i.e., BC, UVPM, and PNC (178–420 nm)) that have relatively large model residuals due to higher measurement uncertainties.

**3.6. Emission Factors.** This study further estimated the annual average fuel-based EFs of three transportation-related sources, shown in Table 2, and compared them to results reported in the literature. For aircraft emission source (factor 1), the EF of BC reached  $2.3 \times 10^{-2}$  g/kg, which is very close to  $4.2 \times 10^{-2}$  g/kg, an average value from several global aviation emission inventories.<sup>122</sup> The EF of aircraft-related NO<sub>x</sub> was 20 g/kg, a bit higher but the same magnitude as the previous studies.<sup>122,123</sup> We note that many studies only reported the NO<sub>x</sub> EF, so it will be larger than the realistic NO<sub>x</sub> EF. Wayson et al. further revealed that the takeoff of aircraft has a higher NO<sub>x</sub> EF than landing,<sup>123</sup> but this study cannot distinguish takeoff emission from those of landing. The aviation EF of PNC was  $2.2 \times 10^{16}$  kg<sup>-1</sup>, consistent with an average of  $3.8 \times 10^{16}$  kg<sup>-1</sup> from the field test of 275 aircraft engine takeoff plumes.<sup>89</sup> For emissions from diesel trucks (factor 2), the EF of BC, NO<sub>x</sub>, and PNC was 0.31, 9.9 g/kg, and  $3.1 \times 10^{16}$  kg<sup>-1</sup>, respectively. All these results were comparable to previous simulation and field studies, except that the EF of PNC was a bit higher in this study,<sup>124–127</sup> possibly due to the regional differences in emission control

technologies of trucks. For gasoline and hybrid passenger vehicles (factor 3), the EF of BC, NO<sub>2</sub>, and PNC was  $1.3 \times 10^{-2}$ , 1.3 g/kg, and  $4.3 \times 10^{12} \text{ kg}^{-1}$ , respectively. Previous studies on gasoline car emissions reported the EFs of these three pollutants as  $1.7 \times 10^{-2}$ , 2.0 g/kg, and 2.2 or  $9.9 \times 10^{13} \text{ kg}^{-1}$ , which agree well with our results.<sup>109,125,126,128</sup> King County Metro Transit also reported that the NO<sub>x</sub> EF of their hybrid buses was 1.6 g/kg, very similar to that of gasoline cars above.<sup>112</sup> All of the above discussion not only provides regional-level estimates of transportation-related EFs for the greater Seattle area between 2019 and 2020, but also validates the source identification in Section 3.2. We note that the difference of PNC EF between this study and previous studies may result from different measurement methods, due to the lack of standards of measuring PNC emissions from gasoline and diesel vehicles in the US, but their results can still provide helpful information for reference. Finally, we can compare these three transportation-related sources and summarize the rankings of different vehicles according to their EFs in Seattle: Diesel truck ≫ Aircraft > Gasoline vehicle (for BC), Aircraft > Diesel truck > Gasoline vehicle (for NO<sub>2</sub>), and Diesel truck > Aircraft ≫ Gasoline vehicle (for PNC). The largest difference exists in EFs of PNC where the EF of aircraft and diesel trucks are three to 4 orders of magnitude higher than that of gasoline cars and hybrid buses.

**3.7. Strengths of This Study.** To the best of our knowledge, this is the first study to combine a one-year mobile monitoring campaign with PMF analysis to simultaneously estimate source-specific air pollution exposures and emission factors of different vehicle types. Compared to previous SAMM studies lasting several days to several months, this study was conducted using a one-year campaign with a time-balanced design. This mobile monitoring design allows us to identify important spatially resolved emission sources with seasonal or diurnal patterns such as residential heating. Therefore, it is very helpful to accurately assess the long-term source-specific air pollution exposures instead of short-term source contributions that are susceptible to some occasional emission events. The mobile monitoring itself can also provide a higher spatial resolution of air pollution and more related source information than that of traditional stationary monitoring stations.

Another feature of this study is the use of a series of external validation approaches to interpret and assess the validity of the PMF results. These included comparing particle size distributions with literature, mapping annual average source contributions in different subgroups, developing LUR models with relevant geospatial covariates, and estimating the ratios between different pollutants in the factor profile. This approach allowed us to correctly categorize transportation-related sources into different vehicle types. This study also considered the particle size distribution of UFPs in addition to mass concentrations of pollutants typically measured in mobile monitoring studies (i.e., PM<sub>2.5</sub>, BC, NO<sub>2</sub>, CO<sub>2</sub>). The particle size can directly help distinguish nucleation mode particles of fresh emissions from those with the accumulation mode. It is also important to assess the source-specific exposure to size-resolved UFPs because this may promote future health-related analyses as it is easier for UFPs with smaller size to enter the human's lung and translocate to other organs, thus adversely impacting human health.

Besides, compared with previous EF estimation methods based on source apportionment, this study considered differences in measurement uncertainties. This also allows for

the development of a long-term average EF at the regional level for various vehicle types separately rather than the EF of individual vehicles in a short period of time.

**3.8. Limitations and Implications for Future Research.** There are still some limitations in this study that can offer valuable insights into future research. First, although this study included different size bins of UFPs, the chemical compositions of particles were not considered, which can also act as important markers for source identification. For transportation-related sources, previous studies considered metal elements (e.g., Cu, Zn, Ba, Sb) and some organic compounds (e.g., *n*-alkanes, hopanes, steranes, polycyclic aromatic hydrocarbons (PAHs)) as the distinctive markers.<sup>129–133</sup> Among the road traffic-related sources, diesel vehicles usually have a lower CO emission factor than gasoline vehicles.<sup>125,134</sup> We note that CO was measured in the campaign but not utilized because it did not meet the quality assurance standards.<sup>20</sup> Gasoline vehicles have been found to emit more PAHs and contribute more to PAHs with high molecular weight, so ratios such as the ratio between indeno(1,2,3-cd) pyrene to the sum of indeno(1,2,3-cd) pyrene and benzo(ghi)perylene were adopted in previous studies.<sup>131,135–137</sup> For secondary aerosols, the measurement of nitrate and sulfate helps identify the secondary inorganic aerosols (SIA) formed from the oxidation of NO<sub>2</sub> and SO<sub>2</sub>.<sup>30</sup> The oil combustion factor obtained in this study is a mixture of several types of oil due to a lack of chemical information. The ratio of Ni to V was a typical tracer for heavy oil combustion from ships.<sup>138,139</sup> However, some researchers found that this tracer does not always work, and proposed other tracers, such as using profiles of *n*-alkanes (C11–C40) and PAHs in size-resolved particles.<sup>140,141</sup> Another potential source of this factor is cooking oil fumes. Previous studies utilized several organic tracers of cooking emissions, such as palmitic acid, stearic acid, cholesterol, and azelaic acid.<sup>142–144</sup> For wood combustion, a series of organic compounds has been considered as useful markers, such as levoglucosan, mannosan, galactosan, dehydroabietic acid, and retene.<sup>129,142,145–150</sup> There may be other sources that were not reported in this study. For example, the sea salt source in the coastal area is marked by the presence of sodium and chloride.<sup>30,151</sup>

Second, this study pooled all spatiotemporal multipollutant stop-level data into one PMF model. Many previous studies have applied PMF to multisite data sets.<sup>152–166</sup> Nevertheless, this approach may still confront challenges when faced with spatiotemporal variation simultaneously, which depends on its inherent assumptions and requires further mathematical validation. On one hand, the PMF model assumes a static factor profile throughout the monitoring campaign, while real-world source profiles may have seasonal variation. A few recent studies have started to apply a seasonal PMF or rolling PMF methods to obtain dynamic profiles.<sup>167,168</sup> However, these dynamic models may need a larger sample size and lead to more complicated factors, which are difficult to interpret. On the other hand, the multisite PMF analysis assumes a constant factor profile across space. Through a simulation study, Tian et al. concluded that the multisite PMF will not be influenced by the spatial correlation between sites if the source profiles are similar between sites, but will be sensitive to high spatial variability of source profiles.<sup>169</sup> It is impractical to apply the PMF model to each of 309 sites with limited repeated measures separately, so we used the randomly selected sites to validate the robustness of the factor profiles in this study.

Third, some pollutants were not predicted very well by the PMF model in this study, such as CO<sub>2</sub> and NO<sub>2</sub>, which suggests additional possible sources not included in the six factors. We mapped the annual average, seasonal average, and rush-/nonrush-hour average scaled residuals of these pollutants, which are discussed in detail in SI1 Section S2.2. Briefly, the unexplained variation of CO<sub>2</sub> may originate from some characteristics of low-developed land use, while that of NO<sub>2</sub> especially around the downtown area may be related to the cold start of vehicles.<sup>170,171</sup> More research is required in the future that can apply the chemical markers or seasonal PMF discussed above.

Fourth, the rich data of the mobile monitoring campaign have not been fully taken advantage of. Only stop-level data were used in this study, but we also collected on-road measurements. It is more challenging to apply the PMF model to this more highly spatiotemporal data set. Healy et al. proposed a possible approach, which obtained the factor contributions to on-road measurements based on the available factor profiles derived from the stop-level data.<sup>33</sup> It is worthwhile for future studies to try to improve this approach.

To sum up, the novel approach in this study can inform the source contributions to air pollution exposure in Seattle. PNC of ultrafine particles with size <18, 18–42, and 42–178 nm was dominated by emissions from aircraft, diesel trucks, and oil/wood combustion in Seattle, respectively. Gasoline & hybrid vehicles contributed the most to CO<sub>2</sub> and NO<sub>2</sub> atmospheric concentrations, while oil and wood combustion contributed the most to BC and UVPM concentrations. This approach can be extended to other metropolitan areas with mobile monitoring data. Future studies can use the detailed source-specific exposure data generated by this approach to enhance epidemiology studies by providing more precise estimates of the long-term exposure to multiple pollutants. The reduction of the health burden can also be discussed under different scenarios of controlling transportation-related emission factors obtained in this study, which is helpful to improve air quality management and policy-making.

## ASSOCIATED CONTENT

### Supporting Information

The Supporting Information is available free of charge at <https://pubs.acs.org/doi/10.1021/acs.est.4c13242>.

Instruments for air pollution mobile monitoring (Section S1), detailed methods of PMF analysis (Section S2), geospatial covariates for land use regression (LUR) models (Section S3), conversion of emission factors in the literature (Section S4), pollutant concentration and factor profile (Section S5), and external validation and factor interpretation (Section S6) ([PDF](#))

Detailed results of source contribution and source-specific exposure for each site ([XLSX](#))

## AUTHOR INFORMATION

### Corresponding Author

Ningrui Liu — Department of Environmental and Occupational Health Sciences, University of Washington, Seattle, Washington 98195, United States;  [orcid.org/0009-0003-1963-5452](https://orcid.org/0009-0003-1963-5452); Email: [liunr24@uw.edu](mailto:liunr24@uw.edu)

## Authors

Rajni Oshan — Department of Environmental and Occupational Health Sciences, University of Washington, Seattle, Washington 98195, United States

Magali Blanco — Department of Environmental and Occupational Health Sciences, University of Washington, Seattle, Washington 98195, United States;  [orcid.org/0000-0002-9998-995X](https://orcid.org/0000-0002-9998-995X)

Lianne Sheppard — Department of Environmental and Occupational Health Sciences, University of Washington, Seattle, Washington 98195, United States; Department of Biostatistics, University of Washington, Seattle, Washington 98195, United States

Edmund Seto — Department of Environmental and Occupational Health Sciences, University of Washington, Seattle, Washington 98195, United States;  [orcid.org/0000-0003-4058-0313](https://orcid.org/0000-0003-4058-0313)

Timothy Larson — Department of Environmental and Occupational Health Sciences, University of Washington, Seattle, Washington 98195, United States; Department of Civil and Environmental Engineering, University of Washington, Seattle, Washington 98195, United States

Elena Austin — Department of Environmental and Occupational Health Sciences, University of Washington, Seattle, Washington 98195, United States;  [orcid.org/0000-0002-4724-1042](https://orcid.org/0000-0002-4724-1042)

Complete contact information is available at:  
<https://pubs.acs.org/10.1021/acs.est.4c13242>

## Notes

The authors declare no competing financial interest.

## ACKNOWLEDGMENTS

This work was funded by the Adult Changes in Thought-Air Pollution (ACT-AP) Study (National Institute of Environmental Health Sciences [NIEHS], National Institute on Aging [NIA], R01ES026187) and the University of Washington Interdisciplinary Center for Exposure, Disease, Genomics, & Environment (NIEHS, 2P30 ES007033-26).

## REFERENCES

- (1) Boogaard, H.; Patton, A. P.; Atkinson, R. W.; Brook, J. R.; Chang, H. H.; Crouse, D. L.; Fussell, J. C.; Hoek, G.; Hoffmann, B.; Kappeler, R.; Joss, M. K.; Ondras, M.; Sagiv, S. K.; Samoli, E.; Shaikh, R.; Smargiassi, A.; Szpiro, A. A.; Van Vliet, E. D. S.; Vienneau, D.; Weuve, J.; Lurmann, F. W.; Forastiere, F. Long-term exposure to traffic-related air pollution and selected health outcomes: A systematic review and meta-analysis. *Environ. Int.* **2022**, *164*, No. 107262.
- (2) Chen, J.; Hoek, G. Long-term exposure to PM and all-cause and cause-specific mortality: A systematic review and meta-analysis. *Environ. Int.* **2020**, *143*, No. 105974.
- (3) Chen, Z. R.; Liu, N. R.; Tang, H.; Gao, X. H.; Zhang, Y. P.; Kan, H. D.; Deng, F. R.; Zhao, B.; Zeng, X. A.; Sun, Y. X.; Qian, H.; Liu, W.; Mo, J. H.; Zheng, X. H.; Huang, C.; Sun, C. J.; Zhao, Z. H. Health effects of exposure to sulfur dioxide, nitrogen dioxide, ozone, and carbon monoxide between 1980 and 2019: A systematic review and meta-analysis. *Indoor Air* **2022**, *32* (11), No. e13170.
- (4) Cheng, I.; Yang, J.; Tseng, C.; Wu, J.; Shariff-Marco, S.; Park, S. L.; Conroy, S. M.; Inamdar, P. P.; Fruin, S.; Larson, T.; Setiawan, V. W.; DeRouen, M. C.; Gomez, S. L.; Wilkens, L. R.; Le Marchand, L.; Stram, D. O.; Samet, J.; Ritz, B.; Wu, A. H. Traffic-related Air Pollution and Lung Cancer Incidence: The California Multiethnic Cohort Study. *Am. J. Respir. Crit. Care Med.* **2022**, *206* (8), 1008–1018.

- (5) Shah, A. S. V.; Lee, K. K.; McAllister, D. A.; Hunter, A.; Nair, H.; Whiteley, W.; Langrish, J. P.; Newby, D. E.; Mills, N. L. Short term exposure to air pollution and stroke: systematic review and meta-analysis. *BMJ* **2015**, *350*, No. h1295.
- (6) GBD 2019 Risk Factors Collaborators. Global burden of 87 risk factors in 204 countries and territories, 1990–2019: a systematic analysis for the Global Burden of Disease Study 2019. *Lancet* **2020**, *396* (10258), 1223–1249.
- (7) Apte, J. S.; Messier, K. P.; Gani, S.; Brauer, M.; Kirchstetter, T. W.; Lunden, M. M.; Marshall, J. D.; Portier, C. J.; Vermeulen, R. C. H.; Hamburg, S. P. High-Resolution Air Pollution Mapping with Google Street View Cars: Exploiting Big Data. *Environ. Sci. Technol.* **2017**, *51* (12), 6999–7008.
- (8) Chen, Y.; Gu, P.; Schulte, N.; Zhou, X.; Mara, S.; Croes, B. E.; Herner, J. D.; Vijayan, A. A new mobile monitoring approach to characterize community-scale air pollution patterns and identify local high pollution zones. *Atmos. Environ.* **2022**, *272*, No. 118936.
- (9) Deshmukh, P.; Kimbrough, S.; Krabbe, S.; Logan, R.; Isakov, V.; Baldauf, R. Identifying air pollution source impacts in urban communities using mobile monitoring. *Sci. Total Environ.* **2020**, *715*, No. 136979.
- (10) Hankey, S.; Marshall, J. D. Land Use Regression Models of On-Road Particulate Air Pollution (Particle Number, Black Carbon, PM<sub>2.5</sub>, Particle Size) Using Mobile Monitoring. *Environ. Sci. Technol.* **2015**, *49* (15), 9194–9202.
- (11) Hatzopoulou, M.; Valois, M. F.; Levy, I.; Mihele, C.; Lu, G.; Bagg, S.; Minet, L.; Brook, J. Robustness of Land-Use Regression Models Developed from Mobile Air Pollutant Measurements. *Environ. Sci. Technol.* **2017**, *51* (7), 3938–3947.
- (12) Kerckhoffs, J.; Hoek, G.; Gehring, U.; Vermeulen, R. Modelling nationwide spatial variation of ultrafine particles based on mobile monitoring. *Environ. Int.* **2021**, *154*, No. 106569.
- (13) Kerckhoffs, J.; Hoek, G.; Messier, K. P.; Brunekreef, B.; Meliefste, K.; Klompmaker, J. O.; Vermeulen, R. Comparison of Ultrafine Particle and Black Carbon Concentration Predictions from a Mobile and Short-Term Stationary Land-Use Regression Model. *Environ. Sci. Technol.* **2016**, *50* (23), 12894–12902.
- (14) Larson, T.; Henderson, S. B.; Brauer, M. Mobile Monitoring of Particle Light Absorption Coefficient in an Urban Area as a Basis for Land Use Regression. *Environ. Sci. Technol.* **2009**, *43* (13), 4672–4678.
- (15) Minet, L.; Liu, R.; Valois, M. F.; Xu, J.; Weichenthal, S.; Hatzopoulou, M. Development and Comparison of Air Pollution Exposure Surfaces Derived from On-Road Mobile Monitoring and Short-Term Stationary Sidewalk Measurements. *Environ. Sci. Technol.* **2018**, *52* (6), 3512–3519.
- (16) Presto, A. A.; Saha, P. K.; Robinson, A. L. Past, present, and future of ultrafine particle exposures in North America. *Atmos. Environ.: X* **2021**, *10*, No. 100109.
- (17) Apte, J. S.; Manchanda, C. High-resolution urban air pollution mapping. *Science* **2024**, *385* (6707), 380–385.
- (18) Kim, S. Y.; Blanco, M. N.; Bi, J.; Larson, T. V.; Sheppard, L. Exposure assessment for air pollution epidemiology: A scoping review of emerging monitoring platforms and designs. *Environ. Res.* **2023**, *223*, No. 115451.
- (19) Blanco, M. N.; Bi, J.; Austin, E.; Larson, T. V.; Marshall, J. D.; Sheppard, L. Impact of Mobile Monitoring Network Design on Air Pollution Exposure Assessment Models. *Environ. Sci. Technol.* **2023**, *57* (1), 440–450.
- (20) Blanco, M. N.; Gassett, A.; Gould, T.; Doubleday, A.; Slager, D. L.; Austin, E.; Seto, E.; Larson, T. V.; Marshall, J. D.; Sheppard, L. Characterization of Annual Average Traffic-Related Air Pollution Concentrations in the Greater Seattle Area from a Year-Long Mobile Monitoring Campaign. *Environ. Sci. Technol.* **2022**, *56* (16), 11460–11472.
- (21) Chambliss, S. E.; Pinon, C. P. R.; Messier, K. P.; LaFranchi, B.; Upperman, C. R.; Lunden, M. M.; Robinson, A. L.; Marshall, J. D.; Apte, J. S. Local- and regional-scale racial and ethnic disparities in air pollution determined by long-term mobile monitoring. *Proc. Natl. Acad. Sci. U.S.A.* **2021**, *118* (37), No. e2109249118.
- (22) Upadhyा, A. R.; Kushwaha, M.; Agrawal, P.; Gingrich, J. D.; Asundi, J.; Sreekanth, V.; Marshall, J. D.; Apte, J. S. Multi-season mobile monitoring campaign of on-road air pollution in Bengaluru, India: High-resolution mapping and estimation of quasi-emission factors. *Sci. Total Environ.* **2024**, *914*, No. 169987.
- (23) Chen, C.; Liu, S.; Dong, W.; Song, Y.; Chu, M. T.; Xu, J. H.; Guo, X. B.; Zhao, B.; Deng, F. R. Increasing cardiopulmonary effects of ultrafine particles at relatively low fine particle concentrations. *Sci. Total Environ.* **2021**, *751*, No. 141726.
- (24) Bouma, F.; Janssen, N. A. H.; Wesseling, J.; van Ratingen, S.; Strak, M.; Kerckhoffs, J.; Gehring, U.; Hendrix, W.; de Hoogh, K.; Vermeulen, R.; Hoek, G. Long-term exposure to ultrafine particles and natural and cause-specific mortality. *Environ. Int.* **2023**, *175*, No. 107960.
- (25) Hopke, P. K.; Croft, D. P.; Zhang, W.; Lin, S.; Masiol, M.; Squizzato, S.; Thurston, S. W.; van Wijngaarden, E.; Utell, M. J.; Rich, D. Q. Changes in the hospitalization and ED visit rates for respiratory diseases associated with source-specific PM(2.5) in New York State from 2005 to 2016. *Environ. Res.* **2020**, *181*, No. 108912.
- (26) Lucht, S.; Hennig, F.; Moebus, S.; Ohlwein, S.; Herder, C.; Kowall, B.; Jockel, K. H.; Hoffmann, B. All-source and source-specific air pollution and 10-year diabetes Incidence: Total effect and mediation analyses in the Heinz Nixdorf recall study. *Environ. Int.* **2020**, *136*, No. 105493.
- (27) Poulsen, A. H.; Sorensen, M.; Hvidtfeldt, U. A.; Christensen, J. H.; Brandt, J.; Frohn, L. M.; Ketzel, M.; Andersen, C.; Raaschou-Nielsen, O. Source-Specific Air Pollution Including Ultrafine Particles and Risk of Myocardial Infarction: A Nationwide Cohort Study from Denmark. *Environ. Health Perspect.* **2023**, *131* (5), No. 57010.
- (28) Rich, D. Q.; Zhang, W.; Lin, S.; Squizzato, S.; Thurston, S. W.; van Wijngaarden, E.; Croft, D.; Masiol, M.; Hopke, P. K. Triggering of cardiovascular hospital admissions by source specific fine particle concentrations in urban centers of New York State. *Environ. Int.* **2019**, *126*, 387–394.
- (29) Agier, L.; Portengen, L.; Chadeau-Hyam, M.; Basagana, X.; Giorgis-Allemand, L.; Siroux, V.; Robinson, O.; Vlaanderen, J.; Gonzalez, J. R.; Nieuwenhuijsen, M. J.; Vineis, P.; Vrijheid, M.; Slama, R.; Vermeulen, R. A Systematic Comparison of Linear Regression-Based Statistical Methods to Assess Exposome-Health Associations. *Environ. Health Perspect.* **2016**, *124* (12), 1848–1856.
- (30) Hopke, P. K.; Dai, Q.; Li, L.; Feng, Y. Global review of recent source apportionments for airborne particulate matter. *Sci. Total Environ.* **2020**, *740*, No. 140091.
- (31) Hopke, P. K.; Feng, Y.; Dai, Q. Source apportionment of particle number concentrations: A global review. *Sci. Total Environ.* **2022**, *819*, No. 153104.
- (32) Argyropoulos, G.; Samara, C.; Voutsas, D.; Kouras, A.; Manoli, E.; Voliotis, A.; Tsakis, A.; Chasapidis, L.; Konstandopoulos, A.; Eleftheriadis, K. Concentration levels and source apportionment of ultrafine particles in road microenvironments. *Atmos. Environ.* **2016**, *129*, 68–78.
- (33) Healy, R. M.; Sofowote, U. M.; Wang, J. M.; Chen, Q.; Todd, A. Spatially Resolved Source Apportionment of Industrial VOCs Using a Mobile Monitoring Platform. *Atmosphere* **2022**, *13* (10), No. 1722.
- (34) Jing, D.; Yang, K.; Shi, Z.; Cai, X.; Li, S.; Li, W.; Wang, Q. Novel approach for identifying VOC emission characteristics based on mobile monitoring platform data and deep learning: Application of source apportionment in a chemical industrial park. *Heliyon* **2024**, *10* (8), No. e29077.
- (35) Kelp, M.; Gould, T.; Austin, E.; Marshall, J. D.; Yost, M.; Simpson, C.; Larson, T. Sensitivity analysis of area-wide, mobile source emission factors to high-emitter vehicles in Los Angeles. *Atmos. Environ.* **2020**, *223*, No. 117212.
- (36) Larson, T.; Gould, T.; Riley, E. A.; Austin, E.; Fintzi, J.; Sheppard, L.; Yost, M.; Simpson, C. Ambient Air Quality Measurements from a Continuously Moving Mobile Platform: Estimation of

- Area-Wide, Fuel-Based, Mobile Source Emission Factors Using Absolute Principal Component Scores. *Atmos. Environ.* **2017**, *152*, 201–211.
- (37) Liao, H.-T.; Chou, C. C. K.; Huang, S.-H.; Lu, C.-J.; Chen, C.-C.; Hopke, P. K.; Wu, C.-F. Source apportionment of PM 2.5 size distribution and composition data from multiple stationary sites using a mobile platform. *Atmos. Res.* **2017**, *190*, 21–28.
- (38) Robinson, E. S.; Shah, R. U.; Messier, K.; Gu, P.; Li, H. Z.; Apte, J. S.; Robinson, A. L.; Presto, A. A. Land-Use Regression Modeling of Source-Resolved Fine Particulate Matter Components from Mobile Sampling. *Environ. Sci. Technol.* **2019**, *53* (15), 8925–8937.
- (39) Shah, R. U.; Robinson, E. S.; Gu, P.; Robinson, A. L.; Apte, J. S.; Presto, A. A. High-spatial-resolution mapping and source apportionment of aerosol composition in Oakland, California, using mobile aerosol mass spectrometry. *Atmos. Chem. Phys.* **2018**, *18* (22), 16325–16344.
- (40) Tessum, M. W.; Larson, T.; Gould, T. R.; Simpson, C. D.; Yost, M. G.; Vedula, S. Mobile and Fixed-Site Measurements To Identify Spatial Distributions of Traffic-Related Pollution Sources in Los Angeles. *Environ. Sci. Technol.* **2018**, *52* (5), 2844–2853.
- (41) Wen, Y.; Wang, H.; Larson, T.; Kelp, M.; Zhang, S.; Wu, Y.; Marshall, J. D. On-highway vehicle emission factors, and spatial patterns, based on mobile monitoring and absolute principal component score. *Sci. Total Environ.* **2019**, *676*, 242–251.
- (42) Yuan, L.; Wang, H.; Gao, Y.; Ren, G.; Lu, Y.; Jing, S.; Tan, W.; Zhu, L.; Shang, Y.; An, J.; Huang, C. Atmospheric gaseous aromatic hydrocarbons in eastern China based on mobile measurements: Spatial distribution, secondary formation potential and source apportionment. *J. Environ. Sci.* **2023**, *130*, 102–113.
- (43) Li, X.; Dallmann, T. R.; May, A. A.; Stanier, C. O.; Grieshop, A. P.; Lipsky, E. M.; Robinson, A. L.; Presto, A. A. Size distribution of vehicle emitted primary particles measured in a traffic tunnel. *Atmos. Environ.* **2018**, *191*, 9–18.
- (44) Saha, P. K.; Zimmerman, N.; Malings, C.; Hauryliuk, A.; Li, Z. J.; Snell, L.; Subramanian, R.; Lipsky, E.; Apte, J. S.; Robinson, A. L.; Presto, A. A. Quantifying high-resolution spatial variations and local source impacts of urban ultrafine particle concentrations. *Sci. Total Environ.* **2019**, *655*, 473–481.
- (45) Vu, T. V.; Delgado-Saborit, J. M.; Harrison, R. M. Review: Particle number size distributions from seven major sources and implications for source apportionment studies. *Atmos. Environ.* **2015**, *122*, 114–132.
- (46) Cepeda, M.; Schoufour, J.; Freak-Poli, R.; Koolhaas, C. M.; Dhana, K.; Bramer, W. M.; Franco, O. H. Levels of ambient air pollution according to mode of transport: a systematic review. *Lancet Public Health* **2017**, *2* (1), e23–e34.
- (47) Kheris, H.; Kelly, C.; Tate, J.; Parslow, R.; Lucas, K.; Nieuwenhuijsen, M. Exposure to traffic-related air pollution and risk of development of childhood asthma: A systematic review and meta-analysis. *Environ. Int.* **2017**, *100*, 1–31.
- (48) Park, S. S.; Kozawa, K.; Fruin, S.; Mara, S.; Hsu, Y. K.; Jakober, C.; Winer, A.; Herner, J. Emission factors for high-emitting vehicles based on on-road measurements of individual vehicle exhaust with a mobile measurement platform. *J. Air Waste Manage. Assoc.* **2011**, *61* (10), 1046–1056.
- (49) Wren, S. N.; Liggio, J.; Han, Y.; Hayden, K.; Lu, G.; Mihele, C. M.; Mittermeier, R. L.; Stroud, C.; Wentzell, J. J. B.; Brook, J. R. Elucidating real-world vehicle emission factors from mobile measurements over a large metropolitan region: a focus on isocyanic acid, hydrogen cyanide, and black carbon. *Atmos. Chem. Phys.* **2018**, *18* (23), 16979–17001.
- (50) Leinonen, V.; Olin, M.; Martikainen, S.; Karjalainen, P.; Mikkonen, S. Challenges and solutions in determining dilution ratios and emission factors from chase measurements of passenger vehicles. *Atmos. Meas. Technol.* **2023**, *16* (21), 5075–5089.
- (51) Liu, B.; Frey, H. C. Variability in Light-Duty Gasoline Vehicle Emission Factors from Trip-Based Real-World Measurements. *Environ. Sci. Technol.* **2015**, *49* (20), 12525–12534.
- (52) Tong, Z.; Li, Y.; Lin, Q.; Wang, H.; Zhang, S.; Wu, Y.; Zhang, K. M. Uncertainty investigation of plume-chasing method for measuring on-road NO<sub>x</sub> emission factors of heavy-duty diesel vehicles. *J. Hazard. Mater.* **2022**, *424* (Pt B), No. 127372.
- (53) Wang, H.; Wu, Y.; Zhang, K. M.; Zhang, S.; Baldauf, R. W.; Snow, R.; Deshmukh, P.; Zheng, X.; He, L.; Hao, J. Evaluating mobile monitoring of on-road emission factors by comparing concurrent PEMS measurements. *Sci. Total Environ.* **2020**, *736*, No. 139507.
- (54) EPA Positive Matrix Factorization (PMF) 5.0 Fundamentals and User Guide; U.S. Environmental Protection Agency, 2014.
- (55) Brown, S. G.; Eberly, S.; Paatero, P.; Norris, G. A. Methods for estimating uncertainty in PMF solutions: Examples with ambient air and water quality data and guidance on reporting PMF results. *Sci. Total Environ.* **2015**, *518*–519, 626–635.
- (56) Paatero, P.; Eberly, S.; Brown, S. G.; Norris, G. A. Methods for estimating uncertainty in factor analytic solutions. *Atmos. Meas. Technol.* **2014**, *7* (3), 781–797.
- (57) Allen, G. A.; Babich, P.; Poirot, R. L. In *Evaluation of a New Approach for Real Time Assessment of Evaluation of a New Approach for Real Time Assessment of Wood Smoke PM*, Proceedings of the Regional and Global Perspectives on Haze: Causes, Consequences, and Controversies, Air and Waste Management Association Visibility Specialty Conference; CiteSeerX, 2004; pp 25–29.
- (58) Kuang, Y.; Shang, J. Changes in light absorption by brown carbon in soot particles due to heterogeneous ozone aging in a smog chamber. *Environ. Pollut.* **2020**, *266*, No. 115273.
- (59) Olson, M. R.; Garcia, M. V.; Robinson, M. A.; Van Rooy, P.; Dietenberger, M. A.; Bergin, M.; Schauer, J. J. Investigation of black and brown carbon multiple-wavelength-dependent light absorption from biomass and fossil fuel combustion source emissions. *J. Geophys. Res.: Atmos.* **2015**, *120* (13), 6682–6697.
- (60) Wang, Y. G.; Hopke, P. K.; Rattigan, O. V.; Chalupa, D. C.; Utell, M. J. Multiple-year black carbon measurements and source apportionment using Delta-C in Rochester, New York. *J. Air Waste Manage. Assoc.* **2012**, *62* (8), 880–887.
- (61) Wang, Y. G.; Hopke, P. K.; Rattigan, O. V.; Xia, X. Y.; Chalupa, D. C.; Utell, M. J. Characterization of Residential Wood Combustion Particles Using the Two-Wavelength Aethalometer. *Environ. Sci. Technol.* **2011**, *45* (17), 7387–7393.
- (62) Iowa Environmental Mesonet ASOS Global METAR Archives, 2024 [https://mesonet.agron.iastate.edu/request/download.phtml?network=WA\\_ASOS](https://mesonet.agron.iastate.edu/request/download.phtml?network=WA_ASOS).
- (63) Hastie, T.; Tibshirani, R.; Friedman, J. *The Elements of Statistical Learning*, 2nd ed.; Springer: New York, USA, 2017.
- (64) Kutner, H.; Nachtsheim, C.; Neter, J.; Li, W. *Applied Linear Statistical Models*, 5th ed.; McGraw-Hill/Irwin: New York, USA, 2005.
- (65) Chong, I.-G.; Jun, C.-H. Performance of some variable selection methods when multicollinearity is present. *Chemometr. Intell. Lab. Syst.* **2005**, *78* (1–2), 103–112.
- (66) Xiong, R.; Li, J.; Zhang, Y.; Zhang, L.; Jiang, K.; Zheng, H.; Kong, S.; Shen, H.; Cheng, H.; Shen, G.; Tao, S. Global brown carbon emissions from combustion sources. *Environ. Sci. Ecotechnol.* **2022**, *12*, No. 100201.
- (67) Zhang, L.; Luo, Z.; Li, Y.; Chen, Y.; Du, W.; Li, G.; Cheng, H.; Shen, G.; Tao, S. Optically Measured Black and Particulate Brown Carbon Emission Factors from Real-World Residential Combustion Predominantly Affected by Fuel Differences. *Environ. Sci. Technol.* **2021**, *55* (1), 169–178.
- (68) Bounakhla, Y.; Benchrif, A.; Costabile, F.; Tahri, M.; El Gourch, B.; El Hassan, E. K.; Zahry, F.; Bounakhla, M. Overview of PM10, PM2.5 and BC and Their Dependent Relationships with Meteorological Variables in an Urban Area in Northwestern Morocco. *Atmosphere* **2023**, *14* (1), No. 162.
- (69) Austin, E.; Xiang, J.; Gould, T. R.; Shirai, J. H.; Yun, S.; Yost, M. G.; Larson, T. V.; Seto, E. Distinct Ultrafine Particle Profiles Associated with Aircraft and Roadway Traffic. *Environ. Sci. Technol.* **2021**, *55* (5), 2847–2858.
- (70) Ježek, I.; Katrašník, T.; Westerdahl, D.; Močnik, G. Black carbon, particle number concentration and nitrogen oxide emission

- factors of random in-use vehicles measured with the on-road chasing method. *Atmos. Chem. Phys.* **2015**, *15* (19), 11011–11026.
- (71) Shirmohammadi, F.; Sowlat, M. H.; Hasheminassab, S.; Saffari, A.; Ban-Weiss, G.; Sioutas, C. Emission rates of particle number, mass and black carbon by the Los Angeles International Airport (LAX) and its impact on air quality in Los Angeles. *Atmos. Environ.* **2017**, *151*, 82–93.
- (72) Wang, J. M.; Jeong, C. H.; Zimmerman, N.; Healy, R. M.; Wang, D. K.; Ke, F.; Evans, G. J. Plume-based analysis of vehicle fleet air pollutant emissions and the contribution from high emitters. *Atmos. Meas. Technol.* **2015**, *8* (8), 3263–3275.
- (73) Pebesma, E. Simple Features for R: Standardized Support for Spatial Vector Data. *R J.* **2018**, *10* (1), 439–446.
- (74) Pebesma, E.; Bivand, R. *Spatial Data Science: with Applications in R*; Chapman and Hall/CRC: Boca Raton, 2023.
- (75) Bivand, R.; Pebesma, E.; Gomez-Rubio, V. *Applied Spatial Data Analysis with R*, 2nd ed.; Springer: New York, 2013.
- (76) Pebesma, E.; Bivand, R. Classes and methods for spatial data in R. *R News* **2005**, *5* (2), 9–13.
- (77) Padgham, M.; Rudis, B.; Lovelace, R.; Salmon, M. osmdata. *J. Open Source Software* **2017**, *2* (14), No. 305.
- (78) Baston, D. exactextractr: Fast Extraction from Raster Datasets using Polygons (Version 0.10.0). 2023.
- (79) Friedman, J.; Hastie, T.; Tibshirani, R. Regularization Paths for Generalized Linear Models via Coordinate Descent. *J. Stat. Software* **2010**, *33* (1), 1–22.
- (80) Tay, J. K.; Narasimhan, B.; Hastie, T. Elastic Net Regularization Paths for All Generalized Linear Models. *J. Stat. Software* **2023**, *106* (1), 1–31.
- (81) Mevik, B. H.; Wehrens, R. The pls package: Principal component and partial least squares regression in R. *J. Stat. Software* **2007**, *18* (2), 1–23.
- (82) Kuhn, M. Building Predictive Models in R Using the caret Package. *J. Stat. Software* **2008**, *28* (5), 1–26.
- (83) Greenwell, B. M.; Boehmke, B. C. Variable Importance Plots—An Introduction to the vip Package. *R J.* **2020**, *12* (1), 343–366.
- (84) Wickham, H. stringr: Simple, Consistent Wrappers for Common String Operations (Version 1.5.1). 2023.
- (85) Hudda, N.; Fruin, S. A. International Airport Impacts to Air Quality: Size and Related Properties of Large Increases in Ultrafine Particle Number Concentrations. *Environ. Sci. Technol.* **2016**, *50* (7), 3362–3370.
- (86) Keeken, M. P.; Moerman, M.; Zandveld, P.; Henzing, J. S.; Hoek, G. Total and size-resolved particle number and black carbon concentrations in urban areas near Schiphol airport (the Netherlands). *Atmos. Environ.* **2015**, *104*, 132–142.
- (87) Masiol, M.; Harrison, R. M.; Vu, T. V.; Beddows, D. C. S. Sources of sub-micrometre particles near a major international airport. *Atmos. Chem. Phys.* **2017**, *17* (20), 12379–12403.
- (88) Möller, K. L.; Thygesen, L. C.; Schipperijn, J.; Loft, S.; Bonde, J. P.; Mikkelsen, S.; Brauer, C. Occupational Exposure to Ultrafine Particles among Airport Employees - Combining Personal Monitoring and Global Positioning System. *PLoS One* **2014**, *9* (9), No. e106671.
- (89) Moore, R. H.; Shook, M. A.; Ziemska, L. D.; DiGangi, J. P.; Winstead, E. L.; Rauch, B.; Jurkat, T.; Thornhill, K. L.; Crosbie, E. C.; Robinson, C.; Shingler, T. J.; Anderson, B. E. Data Descriptor: Take-off engine particle emission indices for in-service aircraft at Los Angeles International Airport. *Sci. Data* **2017**, *4*, No. 170198.
- (90) Riley, E. A.; Gould, T.; Hartin, K.; Fruin, S. A.; Simpson, C. D.; Yost, M. G.; Larson, T. Ultrafine particle size as a tracer for aircraft turbine emissions. *Atmos. Environ.* **2016**, *139*, 20–29.
- (91) Stacey, B. Measurement of ultrafine particles at airports: A review. *Atmos. Environ.* **2019**, *198*, 463–477.
- (92) Westerdahl, D.; Fruin, S. A.; Fine, P. L.; Sioutas, C. The Los Angeles International Airport as a source of ultrafine particles and other pollutants to nearby communities. *Atmos. Environ.* **2008**, *42* (13), 3143–3155.
- (93) Beyersdorf, A. J.; Timko, M. T.; Ziemska, L. D.; Bulzan, D.; Corporan, E.; Herndon, S. C.; Howard, R.; Miake-Lye, R.; Thornhill, K. L.; Winstead, E.; Wey, C.; Yu, Z.; Anderson, B. E. Reductions in aircraft particulate emissions due to the use of Fischer–Tropsch fuels. *Atmos. Chem. Phys.* **2014**, *14* (1), 11–23.
- (94) Fleuti, E.; Ruf, C.; Maraini, S. Ultrafine Particle Concentrations Zurich Approach Runway 14. 2019. Zurich Airport.
- (95) Harrison, R. M.; Beddows, D. C. S.; Alam, M. S.; Singh, A.; Brean, J.; Xu, R. X.; Kotthaus, S.; Grimmond, S. Interpretation of particle number size distributions measured across an urban area during the FASTER campaign. *Atmos. Chem. Phys.* **2019**, *19* (1), 39–55.
- (96) Hofman, J.; Staelens, J.; Cordell, R.; Stroobants, C.; Zikova, N.; Hama, S. M. L.; Wyche, K. P.; Kos, G. P. A.; Van der Zee, S.; Smallbone, K. L.; Weijers, E. P.; Monks, P. S.; Roekens, E. Ultrafine particles in four European urban environments: Results from a new continuous long-term monitoring network. *Atmos. Environ.* **2016**, *136*, 68–81.
- (97) Hudda, N.; Gould, T.; Hartin, K.; Larson, T. V.; Fruin, S. A. Emissions from an International Airport Increase Particle Number Concentrations 4-fold at 10 km Downwind. *Environ. Sci. Technol.* **2014**, *48* (12), 6628–6635.
- (98) Hudda, N.; Simon, M. C.; Zamore, W.; Brugge, D.; Durant, J. L. Aviation Emissions Impact Ambient Ultrafine Particle Concentrations in the Greater Boston Area. *Environ. Sci. Technol.* **2016**, *50* (16), 8514–8521.
- (99) Masiol, M.; Harrison, R. M. Aircraft engine exhaust emissions and other airport-related contributions to ambient air pollution: A review. *Atmos. Environ.* **2014**, *95*, 409–455.
- (100) Masiol, M.; Hopke, P. K.; Felton, H. D.; Frank, B. P.; Rattigan, O. V.; Wurth, M.; LaDuke, G. H. Analysis of major air pollutants and submicron particles in New York City and Long Island. *Atmos. Environ.* **2017**, *148*, 203–214.
- (101) Rivas, I.; Beddows, D. C. S.; Amato, F.; Green, D. C.; Järvi, L.; Hueglin, C.; Reche, C.; Timonen, H.; Fuller, G. W.; Niemi, J. V.; Pérez, N.; Aurela, M.; Hopke, P. K.; Alastuey, A.; Kulmala, M.; Harrison, R. M.; Querol, X.; Kelly, F. J. Source apportionment of particle number size distribution in urban background and traffic stations in four European cities. *Environ. Int.* **2020**, *135*, No. 105345.
- (102) Ban-Weiss, G. A.; Lunden, M. M.; Kirchstetter, T. W.; Harley, R. A. Size-resolved particle number and volume emission factors for on-road gasoline and diesel motor vehicles. *J. Aerosol Sci.* **2010**, *41* (1), 5–12.
- (103) Preble, C. V.; Dallmann, T. R.; Kreisberg, N. M.; Hering, S. V.; Harley, R. A.; Kirchstetter, T. W. Effects of Particle Filters and Selective Catalytic Reduction on Heavy-Duty Diesel Drayage Truck Emissions at the Port of Oakland. *Environ. Sci. Technol.* **2015**, *49* (14), 8864–8871.
- (104) Kim, W. G.; Kim, C. K.; Lee, J. T.; Kim, J. S.; Yun, C. W.; Yook, S. J. Fine particle emission characteristics of a light-duty diesel vehicle according to vehicle acceleration and road grade. *Transp. Res. Part D: Transp. Environ.* **2017**, *53*, 428–439.
- (105) Zhou, L. Y.; Hallquist, ÅM.; Hallquist, M.; Salvador, C. M.; Gaita, S. M.; Sjödin, Å.; Jerksjö, M.; Salberg, H.; Wängberg, I.; Mellqvist, J.; Liu, Q. Y.; Lee, B. P.; Chan, C. K. A transition of atmospheric emissions of particles and gases from on-road heavy-duty trucks. *Atmos. Chem. Phys.* **2020**, *20* (3), 1701–1722.
- (106) Huang, C.; Lou, D. M.; Hu, Z. Y.; Feng, Q.; Chen, Y. R.; Chen, C. H.; Tan, P. Q.; Yao, D. A PEMS study of the emissions of gaseous pollutants and ultrafine particles from gasoline- and diesel-fueled vehicles. *Atmos. Environ.* **2013**, *77*, 703–710.
- (107) Karjalainen, P.; Pirjola, L.; Heikkilä, J.; Lähnde, T.; Tzamkiosis, T.; Ntziachristos, L.; Keskinen, J.; Rönkkö, T. Exhaust particles of modern gasoline vehicles: A laboratory and an on-road study. *Atmos. Environ.* **2014**, *97*, 262–270.
- (108) Lintusaari, H.; Kuuluvainen, H.; Vanhanen, J.; Salo, L.; Portin, H.; Järvinen, A.; Juuti, P.; Hietikko, R.; Teinilä, K.; Timonen, H.; Niemi, J. V.; Rönkkö, T. Sub-23 nm Particles Dominate Non-Volatile Particle Number Emissions of Road Traffic. *Environ. Sci. Technol.* **2023**, *57* (29), 10763–10772.

- (109) Rönkkö, T.; Pirjola, L.; Karjalainen, P.; Simonen, P.; Teinila, K.; Bloss, M.; Salo, L.; Datta, A.; Lal, B.; Hooda, R. K.; Saarikoski, S.; Timonen, H. Exhaust particle number and composition for diesel and gasoline passenger cars under transient driving conditions: Real-world emissions down to 1.5 nm. *Environ. Pollut.* **2023**, *338*, No. 122645.
- (110) Sun, P.; Feng, J. C.; Yang, S.; Wang, C.; Cui, K. X.; Dong, W.; Du, Y. D.; Yu, X. M.; Zhou, J. D. Particulate number and size distribution of dimethyl ether/gasoline combined injection spark ignition engines at medium engine speed and load. *Fuel* **2022**, *313*, No. 122645.
- (111) Yang, B. B.; Liu, L. L.; Jia, S. K.; Zhang, F.; Yao, M. F. Experimental study on particle size distribution of gasoline compression ignition (GCI) at low-load condition. *Fuel* **2021**, *294*, No. 120502.
- (112) King County Metro Transit. *Feasibility of Achieving a Carbon-Neutral or Zero-Emissions Fleet* 2017.
- (113) Vörösmarty, M.; Hopke, P. K.; Salma, I. Attribution of aerosol particle number size distributions to main sources using an 11-year urban dataset. *Atmos. Chem. Phys.* **2024**, *24* (9), 5695–5712.
- (114) Kim, E.; Hopke, P. K.; Larson, T. V.; Covert, D. S. Analysis of ambient particle size distributions using unmix and positive matrix factorization. *Environ. Sci. Technol.* **2004**, *38* (1), 202–209.
- (115) Kotchenruther, R. A. Recent changes in winter PM<sub>2.5</sub> contributions from wood smoke, motor vehicles, and other sources in the Northwest US. *Atmos. Environ.* **2020**, *237*, No. 117724.
- (116) U.S. Census Bureau; American Community Survey, 2019.
- (117) Tanzer, S. E.; Posada, J.; Geraedts, S.; Ramírez, A. Lignocellulosic marine biofuel: Technoeconomic and environmental assessment for production in Brazil and Sweden. *J. Cleaner Prod.* **2019**, *239*, No. 117845.
- (118) Zhai, S. R.; Albritton, D. Airborne particles from cooking oils: Emission test and analysis on chemical and health implications. *Sustainable Cities Soc.* **2020**, *52*, No. 101845.
- (119) Xiang, J. B.; Hu, L. M.; Hao, J. Y.; Wu, S. Q.; Cao, J. P.; Seto, E. Characterization of time- and size-dependent particle emissions and decay from cooking oil fumes in residence: Impacts of various intervention measures. *Build. Simul.* **2023**, *16* (7), 1149–1158.
- (120) Trojanowski, R.; Fthenakis, V. Nanoparticle emissions from residential wood combustion: A critical literature review, characterization, and recommendations. *Renewable Sustainable Energy Rev.* **2019**, *103*, 515–528.
- (121) Friedman, B. Source apportionment of PM(2.5) at two Seattle chemical speciation sites. *J. Air Waste Manage. Assoc.* **2020**, *70* (7), 687–699.
- (122) Zhang, X.; Chen, X.; Wang, J. A number-based inventory of size-resolved black carbon particle emissions by global civil aviation. *Nat. Commun.* **2019**, *10* (1), No. 534.
- (123) Wayson, R.; Fleming, G. *Consideration of Air Quality Impacts By Airplane Operations At or Above 3000 feet AGL*; Federal Aviation Administration, 2000.
- (124) Ban-Weiss, G. A.; Lunden, M. M.; Kirchstetter, T. W.; Harley, R. A. Measurement of Black Carbon and Particle Number Emission Factors from Individual Heavy-Duty Trucks. *Environ. Sci. Technol.* **2009**, *43* (5), 1419–1424.
- (125) Bureau of Transportation Statistics Estimated U.S. Average Vehicle Emissions Rates per Vehicle by Vehicle Type Using Gasoline and Diesel, 2024. <https://www.bts.gov/content/estimated-national-average-vehicle-emissions-rates-vehicle-vehicle-type-using-gasoline-and-diesel>.
- (126) Cai, H.; Burnham, A.; Wang, M. *Updated Emission Factors of Air Pollutants from Vehicle Operations in GREET Using MOVES*; Argonne National Laboratory, 2013.
- (127) Preble, C. V.; Harley, R. A.; Kirchstetter, T. W. *Measuring Real-World Emissions from the On-Road Heavy-Duty Truck Fleet*; California Air Resources Board, 2019.
- (128) Olin, M.; Oikarinen, H.; Marjanen, P.; Mikkonen, S.; Karjalainen, P. High Particle Number Emissions Determined with Robust Regression Plume Analysis (RRPA) from Hundreds of Vehicle Chases. *Environ. Sci. Technol.* **2023**, *57* (24), 8911–8920.
- (129) Padoan, S.; Zappi, A.; Adam, T.; Melucci, D.; Gambaro, A.; Formenton, G.; Popovicheva, O.; Nguyen, D. L.; Schnelle-Kreis, J.; Zimmermann, R. Organic molecular markers and source contributions in a polluted municipality of north-east Italy: Extended PCA-PMF statistical approach. *Environ. Res.* **2020**, *186*, No. 109587.
- (130) Charron, A.; Polo-Rehn, L.; Besombes, J. L.; Golly, B.; Buisson, C.; Chanut, H.; Marchand, N.; Guillaud, G.; Jaffrezo, J. L. Identification and quantification of particulate tracers of exhaust and non-exhaust vehicle emissions. *Atmos. Chem. Phys.* **2019**, *19* (7), S187–S207.
- (131) Pant, P.; Harrison, R. M. Estimation of the contribution of road traffic emissions to particulate matter concentrations from field measurements: A review. *Atmos. Environ.* **2013**, *77*, 78–97.
- (132) Bai, X. X.; Tian, H. Z.; Zhu, C. Y.; Luo, L. N.; Hao, Y.; Liu, S. H.; Guo, Z. H.; Lv, Y. Q.; Chen, D. X.; Chu, B. W.; Wang, S. X.; Hao, J. M. Present Knowledge and Future Perspectives of Atmospheric Emission Inventories of Toxic Trace Elements: A Critical Review. *Environ. Sci. Technol.* **2023**, *57* (4), 1551–1567.
- (133) de Souza, S. L. Q.; Martins, E. M.; Corrêa, S. M.; da Silva, J. L.; de Castro, R. R.; Assed, F. D. Determination of trace elements in the nanometer, ultrafine, fine, and coarse particulate matters in an area affected by light vehicular emissions in the city of Rio de Janeiro. *Environ. Monit. Assess.* **2021**, *193* (2), No. 92.
- (134) Yang, Z. W.; Liu, Y.; Wu, L.; Martinet, S.; Zhang, Y.; Andre, M.; Mao, H. J. Real-world gaseous emission characteristics of Euro 6b light-duty gasoline- and diesel-fueled vehicles. *Transp. Res. Part D: Transp. Environ.* **2020**, *78*, No. 102215.
- (135) Smith, D. J. T.; Harrison, R. M. Concentrations, trends and vehicle source profile of polynuclear aromatic hydrocarbons in the UK atmosphere. *Atmos. Environ.* **1996**, *30* (14), 2513–2525.
- (136) Lough, G. C.; Schauer, J. J.; Park, J. S.; Shafer, M. M.; Deminter, J. T.; Weinstein, J. P. Emissions of metals associated with motor vehicle roadways. *Environ. Sci. Technol.* **2005**, *39* (3), 826–836.
- (137) Ancelet, T.; Davy, P. K.; Trompeter, W. J.; Markwitz, A.; Weatherburn, D. C. Carbonaceous aerosols in an urban tunnel. *Atmos. Environ.* **2011**, *45* (26), 4463–4469.
- (138) Yang, L.; Zhang, Q. J.; Lv, Z.; Zhao, J. B.; Zhao, J.; Zou, C.; Zou, C.; Wei, N.; Wei, N.; Jia, Z. Y.; Jia, Z.; Zhang, Y. J.; Zhang, Y.; Fu, F.; Fu, F.; Lv, J. H.; Lv, J.; Wu, L.; Wu, L.; Wang, T.; Wang, T.; Peng, J. F.; Peng, J.; Mao, H. J. Real world emission characteristics of Chinese fleet and the current situation of underestimated ship emissions. *J. Cleaner Prod.* **2023**, *418*, No. 138107.
- (139) Celo, V.; Dabek-Zlotorzynska, E.; McCurdy, M. Chemical Characterization of Exhaust Emissions from Selected Canadian Marine Vessels: The Case of Trace Metals and Lanthanoids. *Environ. Sci. Technol.* **2015**, *49* (8), 5220–5226.
- (140) Zhang, F.; Chen, Y. J.; Su, P. H.; Cui, M.; Han, Y.; Matthias, V.; Wang, G. H. Variations and characteristics of carbonaceous substances emitted from a heavy fuel oil ship engine under different operating loads. *Environ. Pollut.* **2021**, *284*, No. 117388.
- (141) Yu, G. Y.; Zhang, Y.; Yang, F.; He, B. S.; Zhang, C. G.; Zou, Z.; Yang, X.; Li, N.; Chen, J. Dynamic Ni/V Ratio in the Ship-Emitted Particles Driven by Multiphase Fuel Oil Regulations in Coastal China. *Environ. Sci. Technol.* **2021**, *55* (22), 15031–15039.
- (142) Simoneit, B. R. T. Biomass burning - A review of organic tracers for smoke from incomplete combustion. *Appl. Geochem.* **2002**, *17* (3), 129–162.
- (143) Liu, Z. H.; Su, J. B.; Ma, A. J.; Zhu, A. X.; Liu, P. Y. Study on emission characteristics of tracer pollutants in cooking oil fumes. *Atmos. Pollut. Res.* **2022**, *13* (5), No. 101409.
- (144) Huang, D. D.; Zhu, S. H.; An, J. Y.; Wang, Q. Q.; Qiao, L. P.; Zhou, M.; He, X.; Ma, Y. G.; Sun, Y. L.; Huang, C.; Yu, J. Z.; Zhang, Q. Comparative Assessment of Cooking Emission Contributions to Urban Organic Aerosol Using Online Molecular Tracers and Aerosol Mass Spectrometry Measurements. *Environ. Sci. Technol.* **2021**, *55* (21), 14526–14535.
- (145) Allen, R. W.; Mar, T.; Koenig, J.; Liu, L. J. S.; Gould, T.; Simpson, C.; Larson, T. Changes in lung function and airway

- inflammation among asthmatic children residing in a woodsmoke-impacted urban area. *Inhal. Toxicol.* **2008**, *20* (4), 423–433.
- (146) Elsasser, M.; Crippa, M.; Orasche, J.; DeCarlo, P. F.; Oster, M.; Pitz, M.; Cyrys, J.; Gustafson, T. L.; Pettersson, J. B. C.; Schnelle-Kreis, J.; Prévôt, A. S. H.; Zimmermann, R. Organic molecular markers and signature from wood combustion particles in winter ambient aerosols: aerosol mass spectrometer (AMS) and high time-resolved GC-MS measurements in Augsburg, Germany. *Atmos. Chem. Phys.* **2012**, *12* (14), 6113–6128.
- (147) Jordan, T. B.; Seen, A. J.; Jacobsen, G. E. Levoglucosan as an atmospheric tracer for woodsmoke. *Atmos. Environ.* **2006**, *40* (27), 5316–5321.
- (148) Ramdahl, T. Retene - a Molecular Marker of Wood Combustion in Ambient Air. *Nature* **1983**, *306* (5943), 580–583.
- (149) Shen, G. F.; Tao, S.; Wei, S. Y.; Zhang, Y. Y.; Wang, R.; Wang, B.; Li, W.; Shen, H. Z.; Huang, Y.; Yang, Y. F.; Wang, W.; Wang, X. L.; Simonich, S. L. M. Retene Emission from Residential Solid Fuels in China and Evaluation of Retene as a Unique Marker for Soft Wood Combustion. *Environ. Sci. Technol.* **2012**, *46* (8), 4666–4672.
- (150) Weggler, B. A.; Ly-Verdu, S.; Jennerwein, M.; Sippula, O.; Reda, A. A.; Orasche, J.; Gröger, T.; Jokiniemi, J.; Zimmermann, R. Untargeted Identification of Wood Type-Specific Markers in Particulate Matter from Wood Combustion. *Environ. Sci. Technol.* **2016**, *50* (18), 10073–10081.
- (151) White, W. H. Chemical markers for sea salt in IMPROVE aerosol data. *Atmos. Environ.* **2008**, *42* (2), 261–274.
- (152) Song, Y.; Zhang, Y. H.; Xie, S. D.; Zeng, L. M.; Zheng, M.; Salmon, L. G.; Shao, M.; Slanina, S. Source apportionment of PM2.5 in Beijing by positive matrix factorization. *Atmos. Environ.* **2006**, *40* (8), 1526–1537.
- (153) Srivastava, D.; Xu, J. S.; Vu, T. V.; Liu, D.; Li, L. J.; Fu, P. Q.; Hou, S. Q.; Palmerola, N. M.; Shi, Z. B.; Harrison, R. M. Insight into PM2.5 sources by applying positive matrix factorization (PMF) at urban and rural sites of Beijing. *Atmos. Chem. Phys.* **2021**, *21* (19), 14703–14724.
- (154) Escrig, A.; Monfort, E.; Celades, I.; Querol, X.; Amato, F.; Minguillón, M. C.; Hopke, P. K. Application of Optimally Scaled Target Factor Analysis for Assessing Source Contribution of Ambient PM. *J. Air Waste Manage.* **2009**, *59* (11), 1296–1307.
- (155) Mooibroek, D.; Schaap, M.; Weijers, E. P.; Hoogerbrugge, R. Source apportionment and spatial variability of PM2.5 using measurements at five sites in the Netherlands. *Atmos. Environ.* **2011**, *45* (25), 4180–4191.
- (156) Minguillón, M.; Querol, X.; Baltensperger, U.; Prévôt, A. S. H. Fine and coarse PM composition and sources in rural and urban sites in Switzerland: Local or regional pollution? *Sci. Total Environ.* **2012**, *427*–428, 191–202.
- (157) Minguillón, M. C.; Cirach, M.; Hoek, G.; Brunekreef, B.; Tsai, M.; de Hoogh, K.; Jedynska, A.; Kooter, I. M.; Nieuwenhuijsen, M.; Querol, X. Spatial variability of trace elements and sources for improved exposure assessment in Barcelona. *Atmos. Environ.* **2014**, *89*, 268–281.
- (158) Larsen, B. R.; Gilardoni, S.; Stenström, K.; Niedzialek, J.; Jimenez, J.; Belis, C. A. Sources for PM air pollution in the Po Plain, Italy: II. Probabilistic uncertainty characterization and sensitivity analysis of secondary and primary sources. *Atmos. Environ.* **2012**, *50*, 203–213.
- (159) Ikemori, F.; Uranishi, K.; Asakawa, D.; Nakatsubo, R.; Makino, M.; Kido, M.; Mitamura, N.; Asano, K.; Nonaka, S.; Nishimura, R.; Sugata, S. Source apportionment in PM2.5 in central Japan using positive matrix factorization focusing on small-scale local biomass burning. *Atmos. Pollut. Res.* **2021**, *12* (3), 349–359.
- (160) Zhou, X.; Li, Z. Q.; Zhang, T. J.; Wang, F. T.; Tao, Y.; Zhang, X.; Wang, F. L.; Huang, J.; Cheng, T. T.; Jiang, H. M.; Zheng, C. Y.; Liu, F. Chemical nature and predominant sources of PM10 and PM2.5 from multiple sites on the Silk Road, Northwest China. *Atmos. Pollut. Res.* **2021**, *12* (1), 425–436.
- (161) Cesari, D.; Donatoe, A.; Conte, M.; Contini, D. Inter-comparison of source apportionment of PM10 using PMF and CMB in three sites nearby an industrial area in central Italy. *Atmos. Res.* **2016**, *182*, 282–293.
- (162) Dai, Q.; Hopke, P. K.; Bi, X.; Feng, Y. Improving apportionment of PM2.5 using multisite PMF by constraining G-values with a priori information. *Sci. Total Environ.* **2020**, *736*, No. 139657.
- (163) Liu, B. S.; Song, N.; Dai, Q. L.; Mei, R. B.; Sui, B. H.; Bi, X. H.; Feng, Y. C. Chemical composition and source apportionment of ambient PM2.5 during the non-heating period in Taian, China. *Atmos. Res.* **2016**, *170*, 23–33.
- (164) Tian, Y. Z.; Liu, J. Y.; Han, S. Q.; Shi, X. R.; Shi, G. L.; Xu, H.; Yu, H. F.; Zhang, Y. F.; Feng, Y. C.; Russell, A. G. Spatial, seasonal and diurnal patterns in physicochemical characteristics and sources of PM2.5 in both inland and coastal regions within a megacity in China. *J. Hazard. Mater.* **2018**, *342*, 139–149.
- (165) Dall'Osto, M.; Querol, X.; Amato, F.; Karanasiou, A.; Lucarelli, F.; Nava, S.; Calzolai, G.; Chiari, M. Hourly elemental concentrations in PM2.5 aerosols sampled simultaneously at urban background and road site during SAPUSS - diurnal variations and PMF receptor modelling. *Atmos. Chem. Phys.* **2013**, *13* (8), 4375–4392.
- (166) Masiol, M.; Squizzato, S.; Formenton, G.; Badiuzzaman, K. M.; Hopke, P. K.; Nenes, A.; Pandis, S. N.; Tositti, L.; Benetello, F.; Visin, F.; Pavoni, B. Hybrid multiple-site mass closure and source apportionment of PM2.5 and aerosol acidity at major cities in the Po Valley. *Sci. Total Environ.* **2020**, *704*, No. 135287.
- (167) Chazeau, B.; El Haddad, I.; Canonaco, F.; Temime-Roussel, B.; D'Anna, B.; D'Anna, B.; Gille, G.; Mesbah, B.; Prevot, A. S. H.; Wortham, H. Organic aerosol source apportionment by using rolling positive matrix factorization: Application to a Mediterranean coastal city. *Atmos. Environ.: X* **2022**, *14*, No. 100176.
- (168) Via, M.; Chen, G.; Canonaco, F.; Daellenbach, K. R.; Chazeau, B.; Chebaicheb, H.; Jiang, J. H.; Keernik, H.; Lin, C. S.; Marchand, N.; Marin, C.; O'Dowd, C.; Ovadnevaite, J.; Petit, J. E.; Pikridas, M.; Riffault, V.; Sciare, J.; Slowik, J. G.; Simon, L.; Vasilescu, J.; Zhang, Y. J.; Favez, O.; Prévôt, A. S. H.; Alastuey, A.; Minguillón, M. C. Rolling vs. seasonal PMF: real-world multi-site and synthetic dataset comparison. *Atmos. Meas. Technol.* **2022**, *15* (18), 5479–5495.
- (169) Tian, Y. Z.; Shi, G. L.; Han, B.; Wang, W.; Zhou, X. Y.; Wang, J.; Li, X.; Feng, Y. C. The accuracy of two- and three-way positive matrix factorization models: Applying simulated multisite data sets. *J. Air Waste Manage.* **2014**, *64* (10), 1122–1129.
- (170) Matthaios, V. N.; Kramer, L. J.; Sommariva, R.; Pope, F. D.; Bloss, W. J. Investigation of vehicle cold start primary NO<sub>2</sub> emissions inferred from ambient monitoring data in the UK and their implications for urban air quality. *Atmos. Environ.* **2019**, *199*, 402–414.
- (171) Zare, A.; Stevanovic, S.; Jafari, M.; Verma, P.; Babaie, M.; Yang, L. P.; Rahman, M. M.; Ristovski, Z. D.; Brown, R. J.; Bodisco, T. A. Analysis of cold-start NO<sub>2</sub> and NO<sub>x</sub> emissions, and the NO<sub>2</sub>/NO<sub>x</sub> ratio in a diesel engine powered with different diesel-biodiesel blends. *Environ. Pollut.* **2021**, *290*, No. 118052.